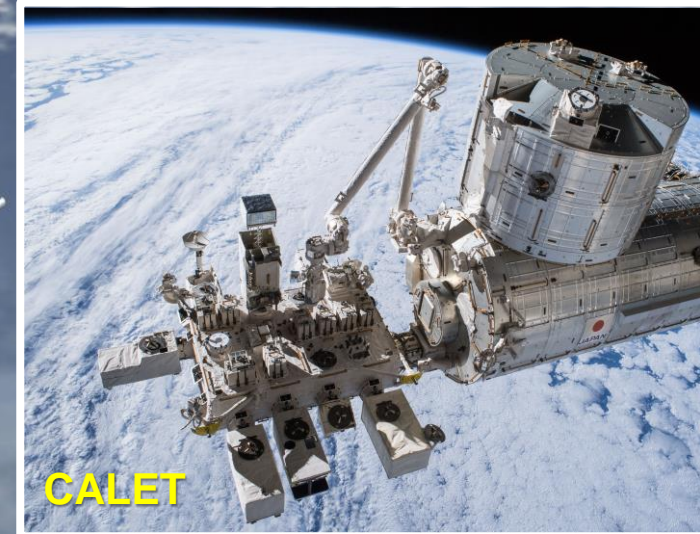
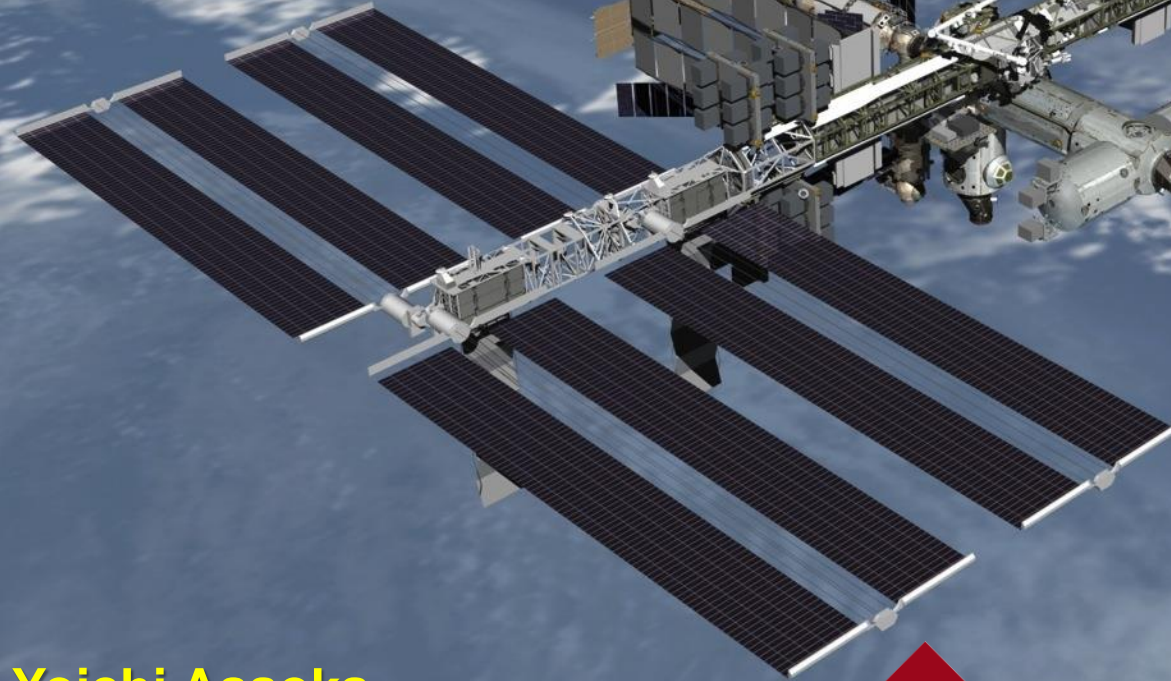




# Recent Results from the CALorimetric Electron Telescope (CALET) on the International Space Station



Yoichi Asaoka  
for the CALET collaboration  
WISE, Waseda University





# CALET Collaboration Team



O. Adriani<sup>25</sup>, Y. Akaike<sup>2</sup>, K. Asano<sup>7</sup>, Y. Asaoka<sup>9,31</sup>, M.G. Bagliesi<sup>29</sup>, E. Berti<sup>25</sup>, G. Bigongiari<sup>29</sup>, W.R. Binns<sup>32</sup>, S. Bonechi<sup>29</sup>, M. Bongio<sup>25</sup>, P. Brogi<sup>29</sup>, A. Bruno<sup>15</sup>, J.H. Buckley<sup>32</sup>, N. Cannady<sup>13</sup>, G. Castellini<sup>25</sup>, C. Checchia<sup>26</sup>, M.L. Cherry<sup>13</sup>, G. Collazuol<sup>26</sup>, V. Di Felice<sup>28</sup>, K. Ebisawa<sup>8</sup>, H. Fuke<sup>8</sup>, T.G. Guzik<sup>13</sup>, T. Hams<sup>3</sup>, N. Hasebe<sup>31</sup>, K. Hibino<sup>10</sup>, M. Ichimura<sup>4</sup>, K. Ioka<sup>34</sup>, W. Ishizaki<sup>7</sup>, M.H. Israel<sup>32</sup>, K. Kasahara<sup>31</sup>, J. Kataoka<sup>31</sup>, R. Kataoka<sup>17</sup>, Y. Katayose<sup>33</sup>, C. Kato<sup>23</sup>, Y. Kawakubo<sup>1</sup>, N. Kawanaka<sup>30</sup>, K. Kohri<sup>12</sup>, H.S. Krawczynski<sup>32</sup>, J.F. Krizmanic<sup>2</sup>, T. Lomtadze<sup>27</sup>, P. Maestro<sup>29</sup>, P.S. Marrocchesi<sup>29</sup>, A.M. Messineo<sup>27</sup>, J.W. Mitchell<sup>15</sup>, S. Miyake<sup>5</sup>, A.A. Moiseev<sup>3</sup>, K. Mori<sup>9,31</sup>, M. Mori<sup>20</sup>, N. Mori<sup>25</sup>, H.M. Motz<sup>31</sup>, K. Munakata<sup>23</sup>, H. Murakami<sup>31</sup>, S. Nakahira<sup>9</sup>, J. Nishimura<sup>8</sup>, G.A De Nolfo<sup>15</sup>, S. Okuno<sup>10</sup>, J.F. Ormes<sup>25</sup>, S. Ozawa<sup>31</sup>, L. Pacini<sup>25</sup>, F. Palma<sup>28</sup>, V. Pal'shin<sup>1</sup>, P. Papini<sup>25</sup>, A.V. Penacchioni<sup>29</sup>, B.F. Rauch<sup>32</sup>, S.B. Ricciarini<sup>25</sup>, K. Sakai<sup>3</sup>, T. Sakamoto<sup>1</sup>, M. Sasaki<sup>3</sup>, Y. Shimizu<sup>10</sup>, A. Shiomi<sup>18</sup>, R. Sparvoli<sup>28</sup>, P. Spillantini<sup>25</sup>, F. Stolz<sup>29</sup>, S. Sugita<sup>1</sup>, J.E. Suh<sup>29</sup>, A. Sulaj<sup>29</sup>, I. Takahashi<sup>11</sup>, M. Takayanagi<sup>8</sup>, M. Takita<sup>7</sup>, T. Tamura<sup>10</sup>, N. Tateyama<sup>10</sup>, T. Terasawa<sup>7</sup>, H. Tomida<sup>8</sup>, S. Torii<sup>31</sup>, Y. Tunesada<sup>19</sup>, Y. Uchihori<sup>16</sup>, S. Ueno<sup>8</sup>, E. Vannuccini<sup>25</sup>, J.P. Wefel<sup>13</sup>, K. Yamaoka<sup>14</sup>, S. Yanagita<sup>6</sup>, A. Yoshida<sup>1</sup>, and K. Yoshida<sup>22</sup>

- 1) Aoyama Gakuin University, Japan
- 2) CRESST/NASA/GSFC and Universities Space Research Association, USA
- 3) CRESST/NASA/GSFC and University of Maryland, USA
- 4) Hirosaki University, Japan
- 5) Ibaraki National College of Technology, Japan
- 6) Ibaraki University, Japan
- 7) ICRR, University of Tokyo, Japan
- 8) ISAS/JAXA Japan
- 9) JAXA, Japan
- 10) Kanagawa University, Japan
- 11) Kavli IPMU, University of Tokyo, Japan
- 12) KEK, Japan
- 13) Louisiana State University, USA
- 14) Nagoya University, Japan
- 15) NASA/GSFC, USA
- 16) National Inst. of Radiological Sciences, Japan
- 17) National Institute of Polar Research, Japan

- 18) Nihon University, Japan
- 19) Osaka City University, Japan
- 20) Ritsumeikan University, Japan
- 21) Saitama University, Japan
- 22) Shibaura Institute of Technology, Japan
- 23) Shinshu University, Japan
- 24) University of Denver, USA
- 25) University of Florence, IFAC (CNR) and INFN, Italy
- 26) University of Padova and INFN, Italy
- 27) University of Pisa and INFN, Italy
- 28) University of Rome Tor Vergata and INFN, Italy
- 29) University of Siena and INFN, Italy
- 30) University of Tokyo, Japan
- 31) Waseda University, Japan
- 32) Washington University-St. Louis, USA
- 33) Yokohama National University, Japan
- 34) Yukawa Institute for Theoretical Physics, Kyoto University, Japan



# CALET Collaboration Team



O. Adriani<sup>25</sup>, Y. Akaike<sup>2</sup>, K. Asano<sup>7</sup>, Y. Asaoka<sup>9,31</sup>, M.G. Bagliesi<sup>29</sup>, E. Berti<sup>25</sup>, G. Bigongiari<sup>29</sup>, W.R. Binns<sup>32</sup>, S. Bonechi<sup>29</sup>, M. Bongio<sup>25</sup>, P. Brogi<sup>29</sup>, A. Bruno<sup>15</sup>, J.H. Buckley<sup>32</sup>, N. Cannady<sup>13</sup>, G. Castellini<sup>25</sup>, C. Checchia<sup>26</sup>, M.L. Cherry<sup>13</sup>, G. Collazuol<sup>26</sup>, V. Di Felice<sup>28</sup>, K. Ebisawa<sup>8</sup>, H. Fuke<sup>8</sup>, T.G. Guzik<sup>13</sup>, T. Hams<sup>3</sup>, N. Hasebe<sup>31</sup>, K. Hibino<sup>10</sup>, M. Ichimura<sup>4</sup>, K. Ioka<sup>34</sup>, W. Ishizaki<sup>7</sup>, M.H. Israel<sup>32</sup>, K. Kasahara<sup>31</sup>, J. Kataoka<sup>31</sup>, R. Kataoka<sup>17</sup>, Y. Katayose<sup>33</sup>, C. Kato<sup>23</sup>, Y. Kawakubo<sup>1</sup>, N. Kawanaka<sup>30</sup>, K. Kohri<sup>12</sup>, H.S. Krawczynski<sup>32</sup>, J.F. Krizmanic<sup>2</sup>, T. Lomtadze<sup>27</sup>, P. Maestro<sup>29</sup>, P.S. Marrocchesi<sup>29</sup>, A.M. Messineo<sup>27</sup>, J.W. Mitchell<sup>15</sup>, S. Miyake<sup>5</sup>, A.A. Moiseev<sup>3</sup>, K. Mori<sup>9,31</sup>, M. Mori<sup>20</sup>, N. Mori<sup>25</sup>, H.M. Motz<sup>31</sup>, K. Munakata<sup>23</sup>, H. Murakami<sup>31</sup>, S. Nakahira<sup>9</sup>, J. Nishimura<sup>8</sup>, G.A De Nolfo<sup>15</sup>, S. Okuno<sup>10</sup>, J.F. Ormes<sup>25</sup>, S. Ozawa<sup>31</sup>, L. Pacini<sup>25</sup>, F. Palma<sup>28</sup>, V. Pal'shin<sup>1</sup>, P. Papini<sup>25</sup>, A.V. Penacchioni<sup>29</sup>, B.F. Rauch<sup>32</sup>, S.B. Ricciarini<sup>25</sup>, K. Sakai<sup>3</sup>, T. Sakamoto<sup>1</sup>, M. Sasaki<sup>3</sup>, Y. Shimizu<sup>10</sup>, A. Shiomi<sup>18</sup>, R. Sparvoli<sup>28</sup>, P. Spillantini<sup>25</sup>, F. Stolz<sup>29</sup>, S. Sugita<sup>1</sup>, J.E. Suh<sup>29</sup>, A. Sulaj<sup>29</sup>, I. Takahashi<sup>11</sup>, M. Takayanagi<sup>8</sup>, M. Takita<sup>7</sup>, T. Tamura<sup>10</sup>, N. Tateyama<sup>10</sup>, T. Terasawa<sup>7</sup>, H. Tomida<sup>8</sup>, S. Torii<sup>31</sup>, Y. Tunesada<sup>19</sup>, Y. Uchihori<sup>16</sup>, S. Ueno<sup>8</sup>, E. Vannuccini<sup>25</sup>, J.P. Wefel<sup>13</sup>, K. Yamaoka<sup>14</sup>, S. Yanagita<sup>6</sup>, A. Yoshida<sup>1</sup>, and K. Yoshida<sup>22</sup>





# Outline

## 1. Introduction

## 2. Calibration

## 3. Operations

## 4. Results

### — Electrons

### — Hadrons

### — Gamma-Rays

### — Space Weather

## 5. Summary

Y.Asaoka, Y.Akaike, Y.Komiya, R.Miyata, S.Torii et al.  
(CALET Collaboration), *Astropart. Phys.* 91 (2017) 1.

Y.Asaoka, S.Ozawa, S.Torii et al.  
(CALET Collaboration), *Astropart. Phys.* 100 (2018) 29.

O.Adriani et al. (CALET Collaboration),  
*Phys.Rev.Lett.* 119 (2017) 181101.

O.Adriani et al. (CALET Collaboration),  
*Phys.Rev.Lett.* 120 (2018) 261102.

O.Adriani et al. (CALET Collab.), *ApJL* 829 (2016) L20.

O.Adriani et al. (CALET Collab.), *ApJ* 863 (2018) 160.

N.Cannady, Y.Asaoka et al. (CALET Collab.),  
*ApJS* 238 (2018) 5.

R.Kataoka et al., *JGR*,  
10.1002/2016GL068930 (2016).

# ISS as Cosmic Ray Observatory



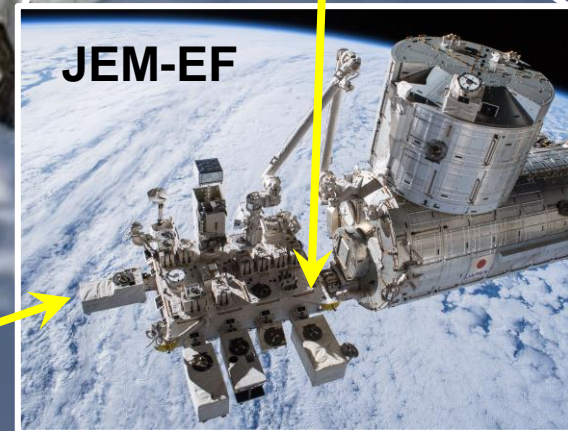
AMS Launch  
May 16, 2011



ISS-CREAM Launch  
August 14, 2017



CALET Launch  
August 19, 2015



JEM-EF

# ISS as Cosmic Ray Observatory



AMS Launch  
May 16, 2011

## Magnet Spectrometer

- Various PID
- Anti-particles
- $E \leq \text{TeV}$

## Calorimeter

- Carbon target
- Hadrons
- Including TeV region



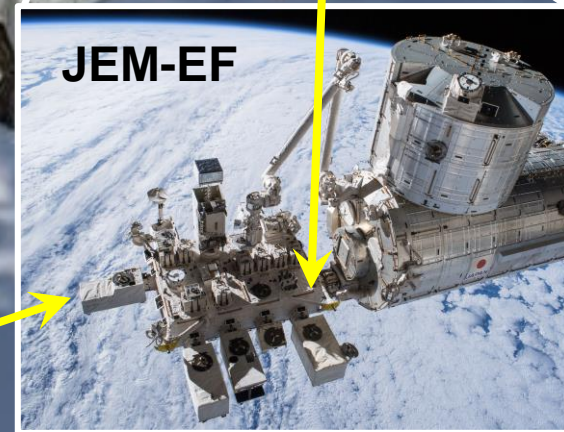
ISS-CREAM Launch  
August 14, 2017

## Calorimeter

- Fully active
- Electrons
- Including TeV region



CALET Launch  
August 19, 2015

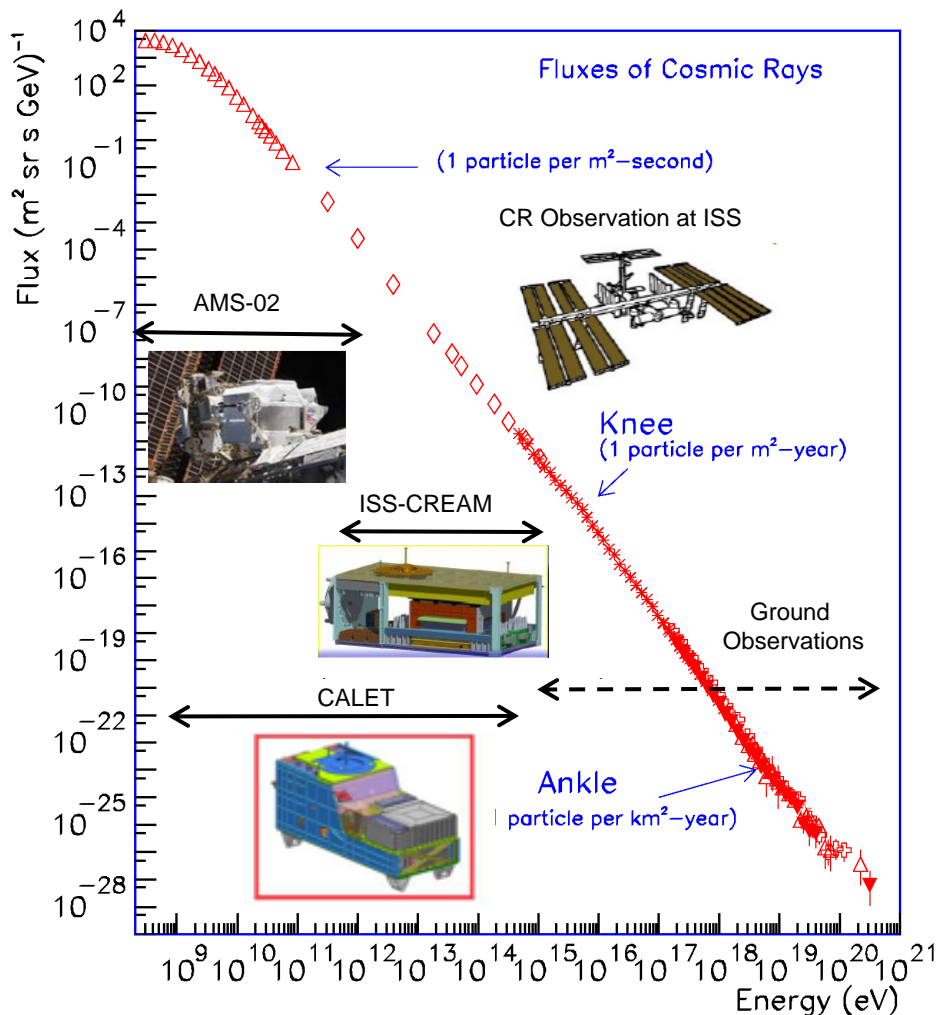


JEM-EF



# Cosmic Ray Observations at the ISS and CALET

## Overview of CALET Observations



□ Direct cosmic ray observations in space at the highest energy region by combining:

- ✓ A large-size detector
- ✓ Long-term observation onboard the ISS (5 years or more is expected)

□ Electron observation in 1 GeV - 20 TeV will be achieved with high energy resolution due to optimization for electron detection

⇒ Search for Dark Matter and Nearby Sources

□ Observation of cosmic-ray nuclei will be performed in energy region from 10 GeV to 1 PeV

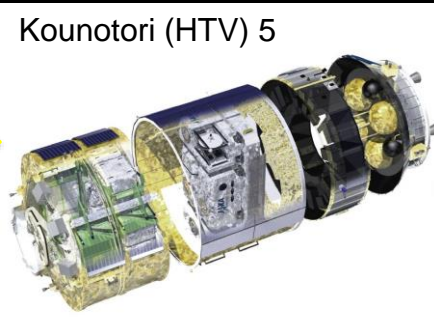
⇒ Unravelling the CR acceleration and propagation mechanism

□ Detection of transient phenomena is expected in space by long-term stable observations

⇒ EM radiation from GW sources, Gamma-ray burst, Solar flare, etc.



# CALET Payload

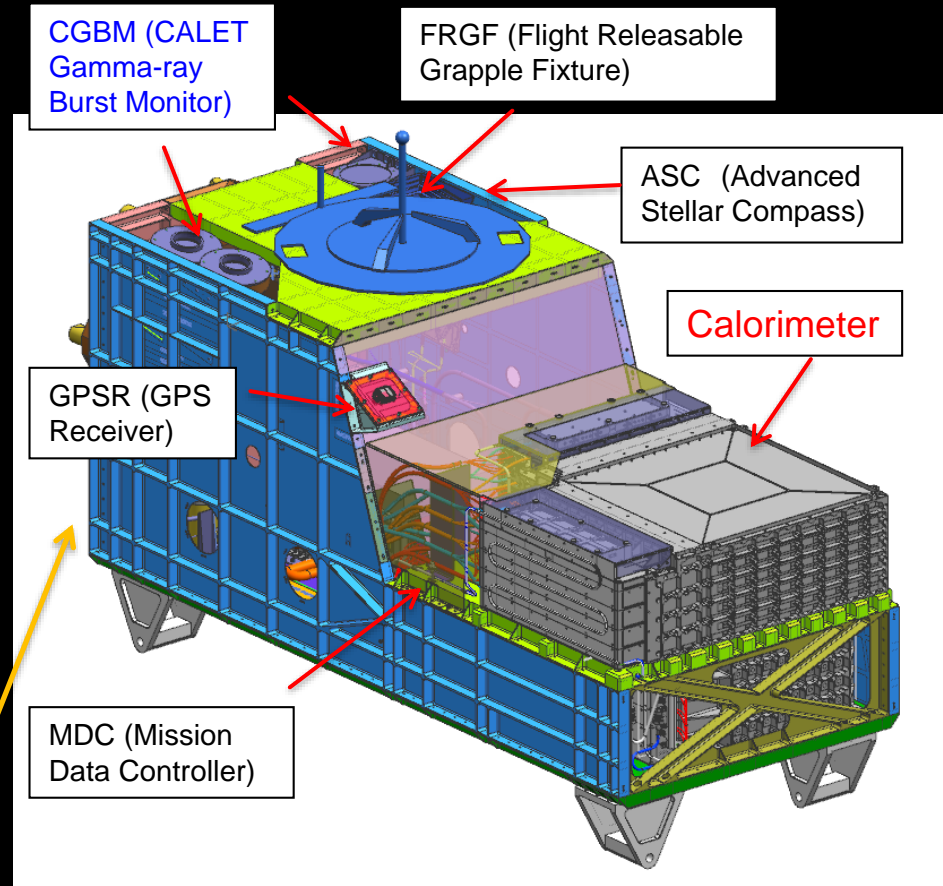


Kounotori (HTV) 5

Launched on Aug. 19<sup>th</sup>, 2015 by the Japanese H2-B rocket

Emplaced on JEM-EF port #9 on Aug. 25<sup>th</sup>, 2015 (JEM-EF: Japanese Experiment Module-Exposed Facility)

JEM/Port #9

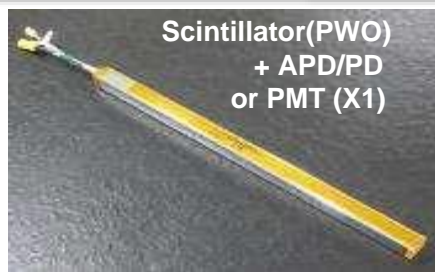


- Mass: 612.8 kg
- JEM Standard Payload Size: 1850mm(L) × 800mm(W) × 1000mm(H)
- Power Consumption: 507 W (max)
- Telemetry: Medium 600 kbps (6.5GB/day) / Low 50 kbps

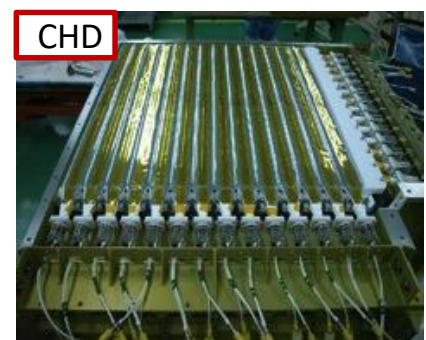
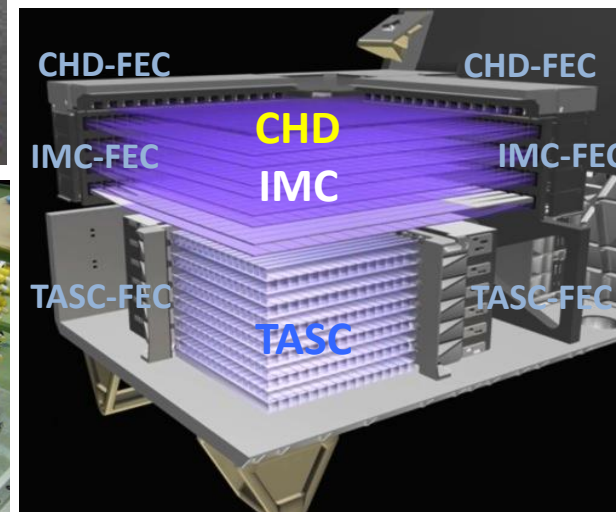




# CALET Instrument



## CALORIMETER

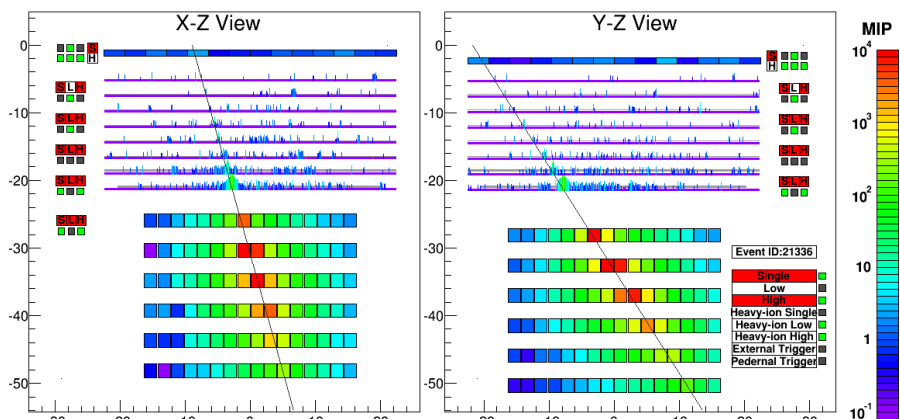


|                        | CHD<br>(Charge Detector)  | IMC<br>(Imaging Calorimeter)  | TASC<br>(Total Absorption Calorimeter)  |
|------------------------|---|---|---|
| Measure                | Charge (Z=1-40)   | Tracking , Particle ID  | Energy, e/p Separation  |
| Geometry<br>(Material) | Plastic Scintillator<br>14 paddles x 2 layers (X,Y): 28 paddles<br>Paddle Size: 32 x 10 x 450 mm <sup>3</sup> | 448 Scifi x 16 layers (X,Y) : 7168 Scifi<br>7 W layers (3X <sub>0</sub> ): 0.2X <sub>0</sub> x 5 + 1X <sub>0</sub> x2<br>Scifi size : 1 x 1 x 448 mm <sup>3</sup> | 16 PWO logs x 12 layers (x,y): 192 logs<br>log size: 19 x 20 x 326 mm <sup>3</sup><br>Total Thickness : 27 X <sub>0</sub> , ~1.2 λ <sub>i</sub> |
| Readout                | PMT+CSA   | 64-anode PMT+ ASIC  | APD/PD+CSA<br>PMT+CSA (for Trigger)@top layer   |



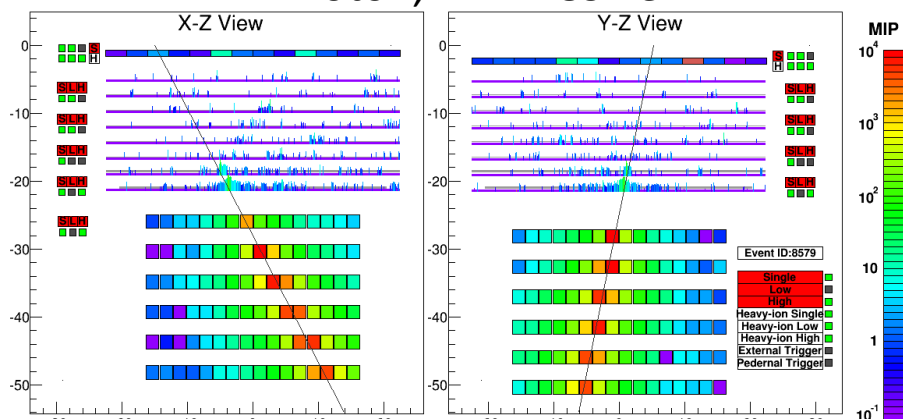
# Event Examples of High-Energy Showers

## Electron, $E=3.05$ TeV



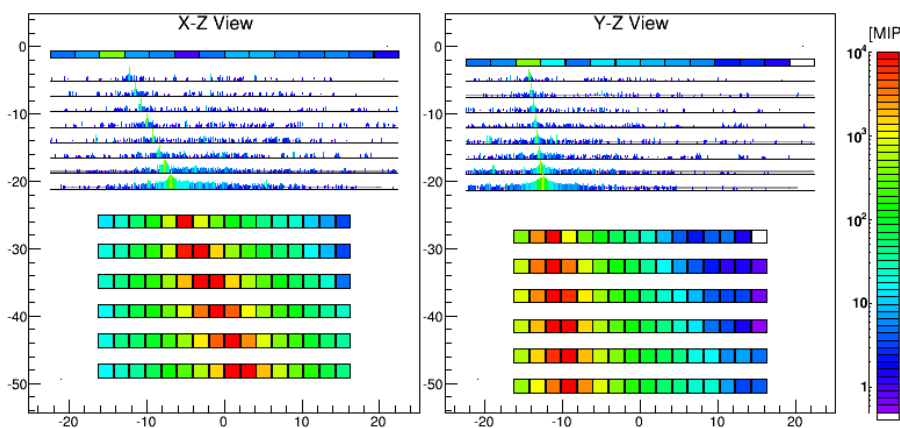
fully contained even at 3TeV

## Proton, $\Delta E=2.89$ TeV



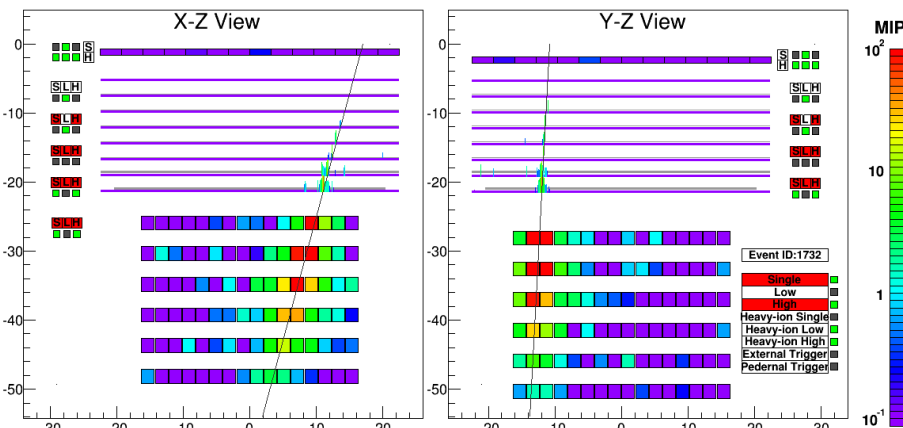
clear difference from electron shower

## Fe( $Z=26$ ), $\Delta E=9.3$ TeV



energy deposit in CHD consistent with Fe

## Gamma-ray, $E=44.3$ GeV



no energy deposit before pair production



# Energy Calibration Using “MIP” in Flight with Tests on Ground

**Intrinsic Advantage of the Fully Active Total Absorption Calorimeter:  
EM Shower Energy Measurement = Energy Deposit Sum × “Small” Correction**

- ❑ **Active and thick calorimeter** absorbs most of the electromagnetic energy (~95%) up to the TeV region in the case of CALET instrument.
- ❑ In principle, **energy measurement with small systematic error** is possible.
- ❑ CALET Detector features:
  - Fine energy resolution of ~ 2 %
  - Wide dynamic range to measure shower energy from 1GeV to 1000 TeV.
- ❑ It requires to obtain **the ADC unit to energy conversion factor** and to calibrate **the whole dynamic range channel by channel**.

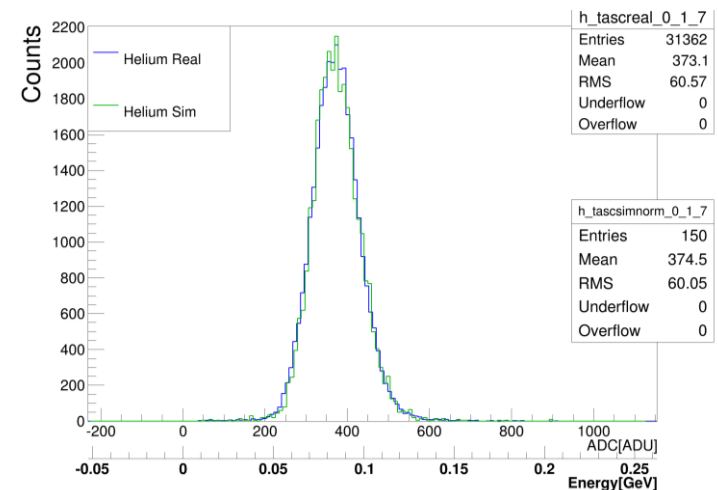
On orbit : Energy conversion factor using “MIP” of p or He

- Position and temperature dependence
- Latitude dependence due to rigidity cutoff

On ground: Linearity measurements for the whole dynamic range

- CHD/IMC – Charge injection
- TASC – UV Laser irradiation (end-to-end)

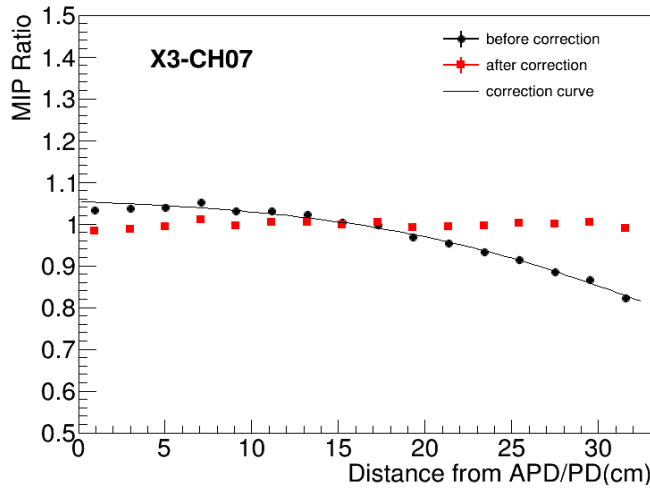
“MIP” peak in PWO: Obs. vs. MC





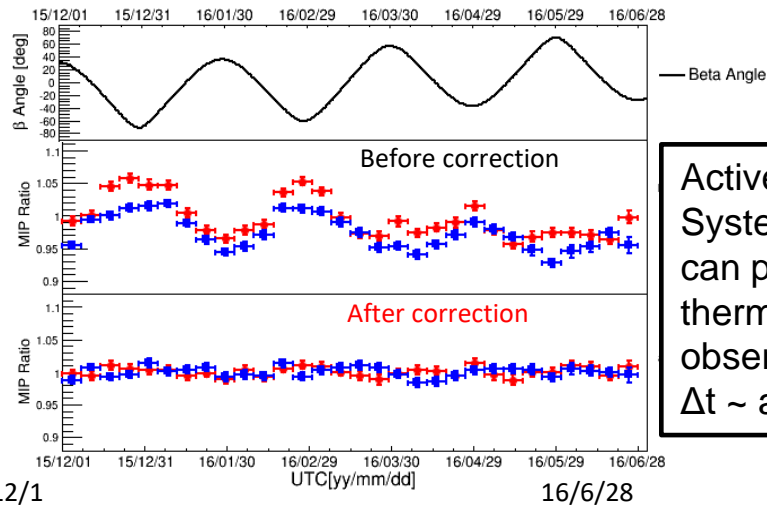
# Position and Temperature Calibration, and Long-term Stability

Example of position dependence correction



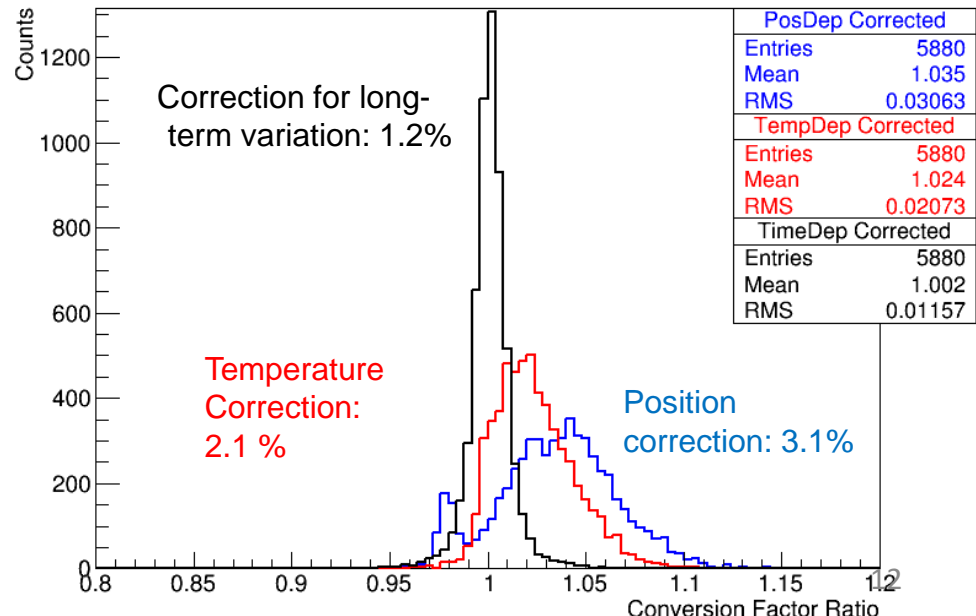
15/12/1

Examples of temperature change correction

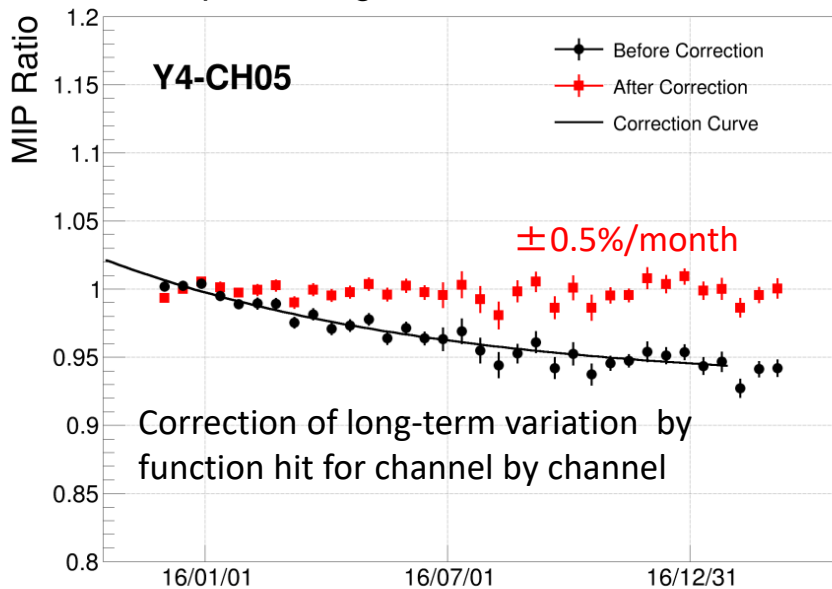


Active Thermal Control System (ATCS) on ISS can provide very stable thermal condition during observations:  
 $\Delta t \sim$  a few degrees

Distribution of MIPs for 192 ch x 16 segmented positions after each correction



Example of long-term variation correction

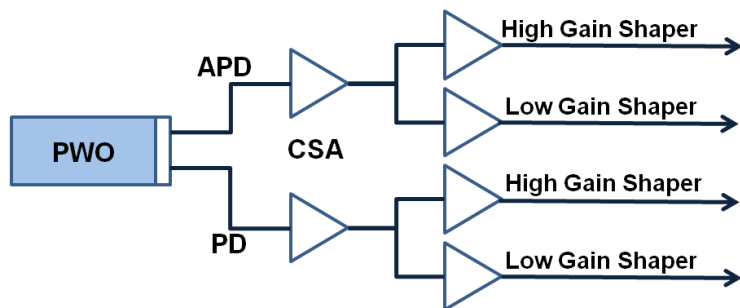
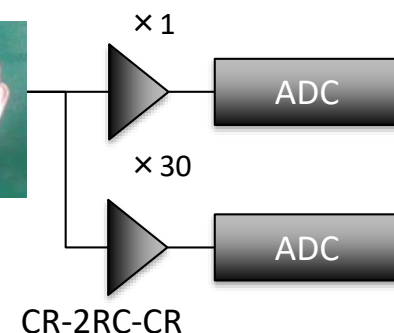


UTC

# Energy Measurement in Dynamic Range of 1-10<sup>6</sup> MIP in TASC



APD gain ~ 50



The linearity was calibrated by using **UV laser irradiation** on ground :

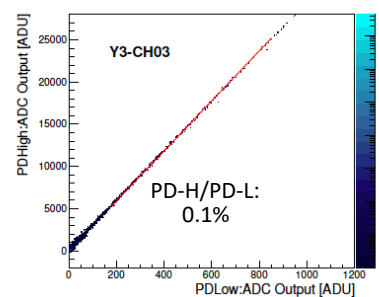
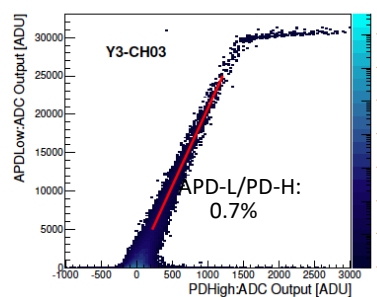
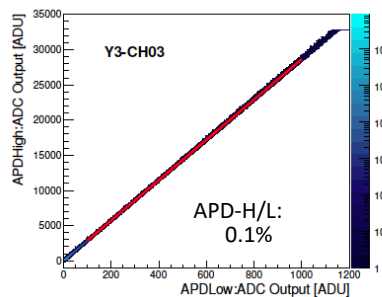
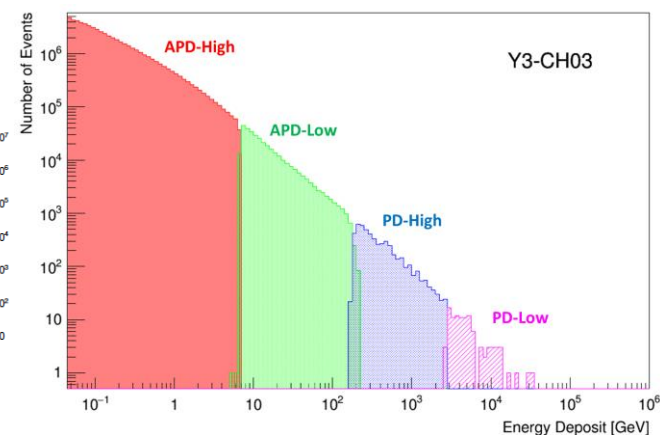
- 1) The linearity is confirmed in the range of 1.4-2.5 %.
- 2) The whole dynamic range is confirmed to cover from 1 MIP to 10<sup>6</sup> MIPs.

| APD-H | APD-L | PD-H | PD-L |
|-------|-------|------|------|
| 1.4%  | 1.5%  | 2.5% | 2.2% |

The correlation between adjacent gain ranges is calibrated by using **in-flight data** in each channel.

| APD-H<br>APD-L | APD-L<br>PD-H | PD-H<br>PD-L |
|----------------|---------------|--------------|
| 0.1%           | 0.7%          | 0.1%         |

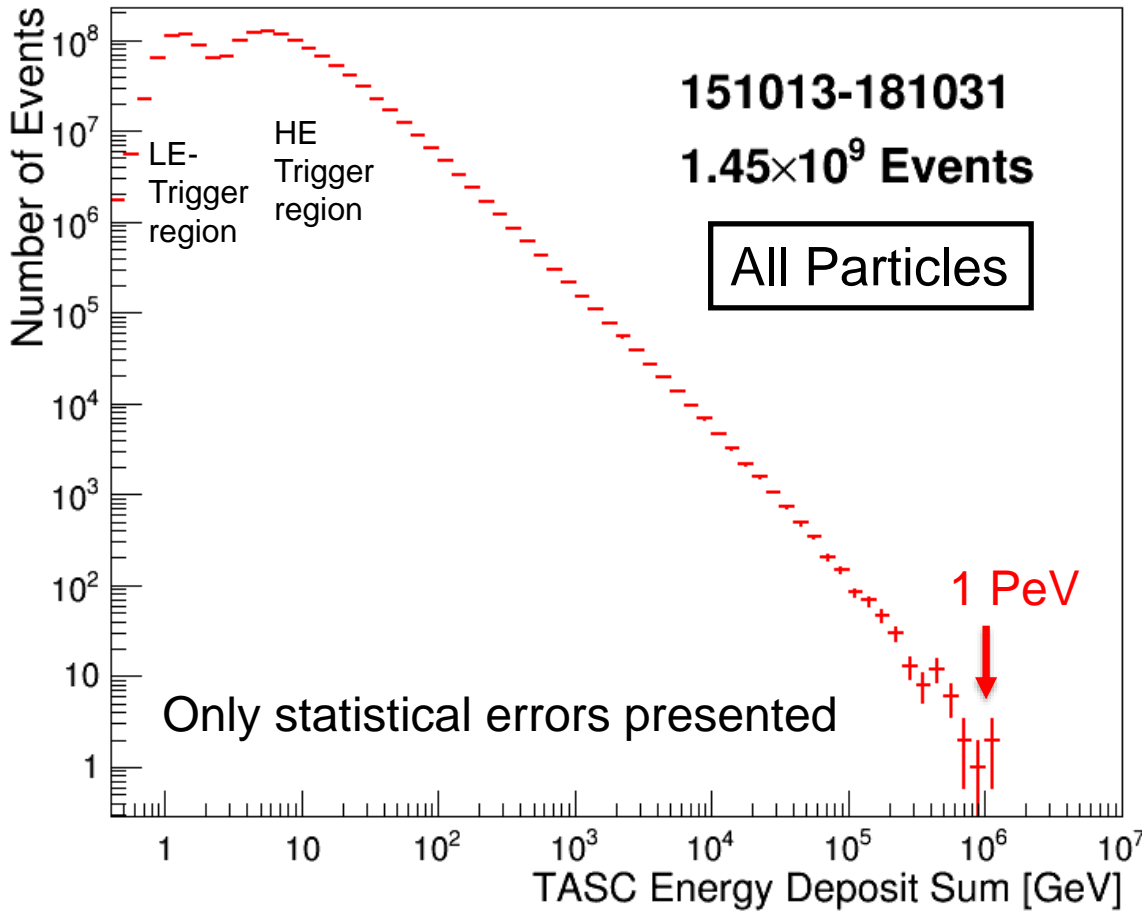
Example of energy distribution in one PWO log



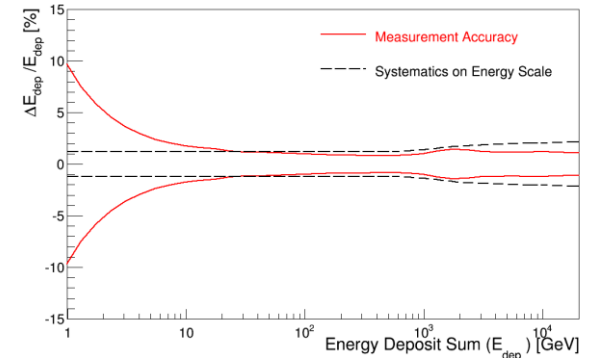


# Energy Deposit Distribution of All Triggered-Events

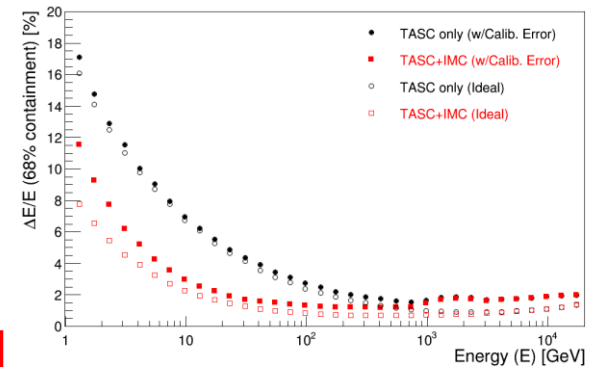
## Distribution of deposit energies ( $\Delta E$ ) in TASC



## Performance of energy measurement in 1GeV-20TeV



## Energy resolution for electrons (TASC+IMC): < 3% over 10 GeV; < 2% over 20GeV

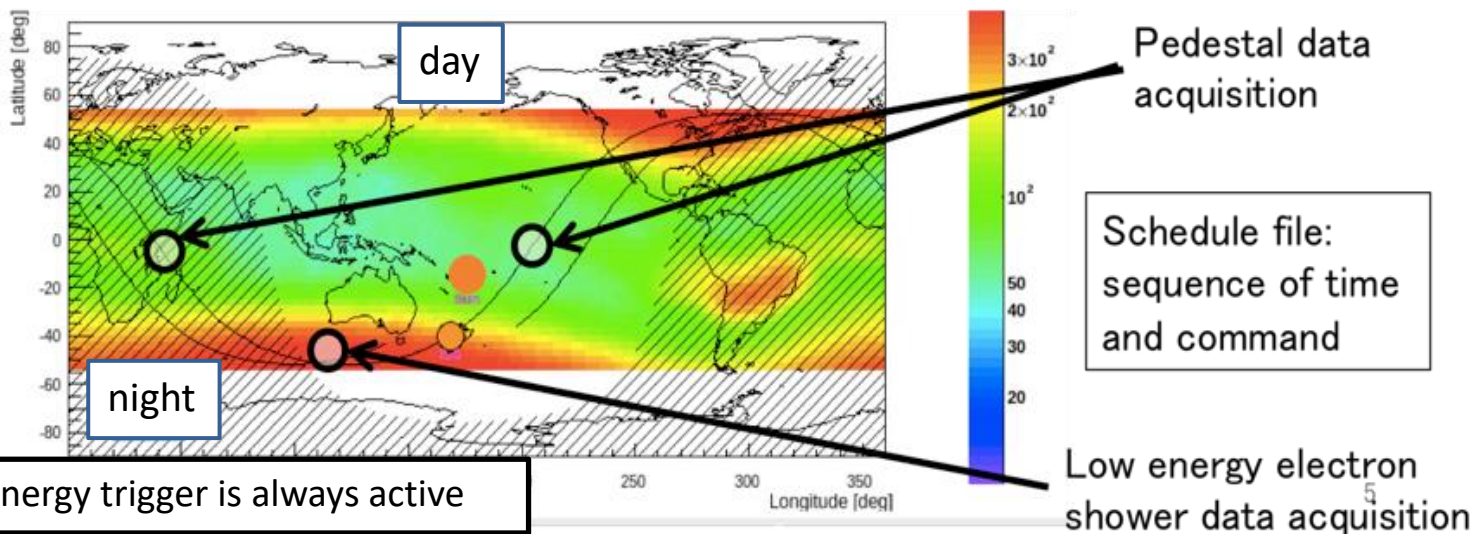


The TASC energy measurements have successfully been carried out in the dynamic range of 1 GeV – 1 PeV.



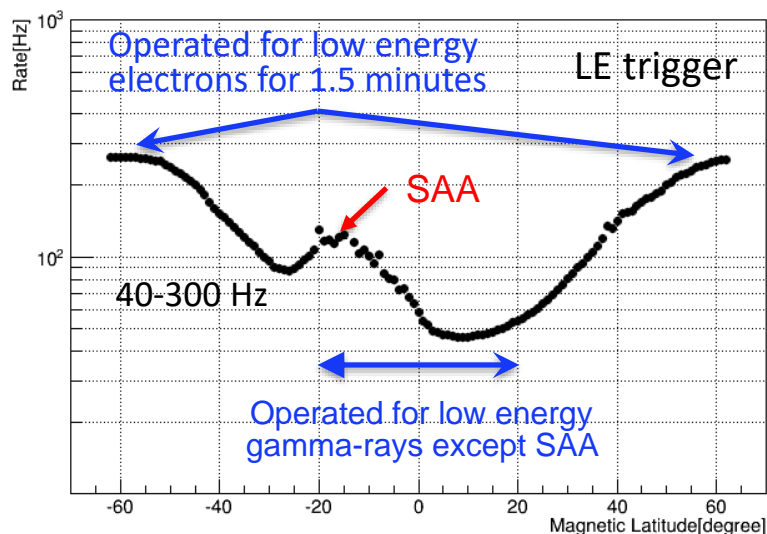
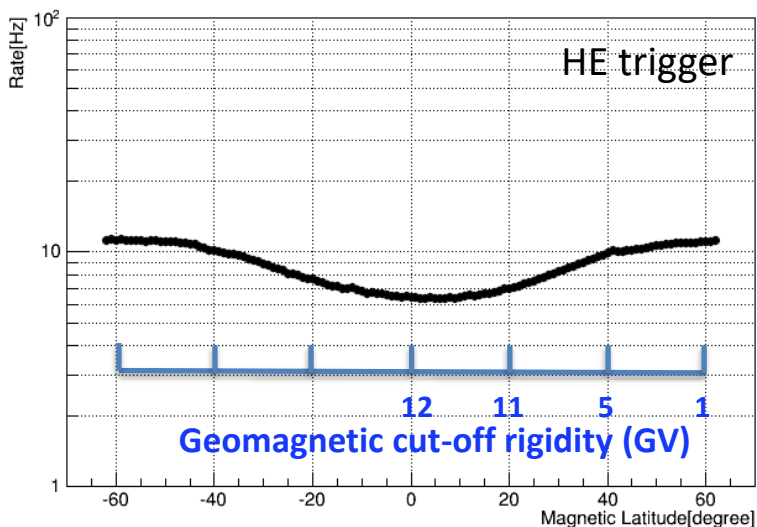
# ISS Orbit and CALET On-orbit Operations

ISS orbit: inclination 51.6 degree, ~400 km



Concept of on-orbit operations

## Dependence of the count rate on geomagnetic latitude

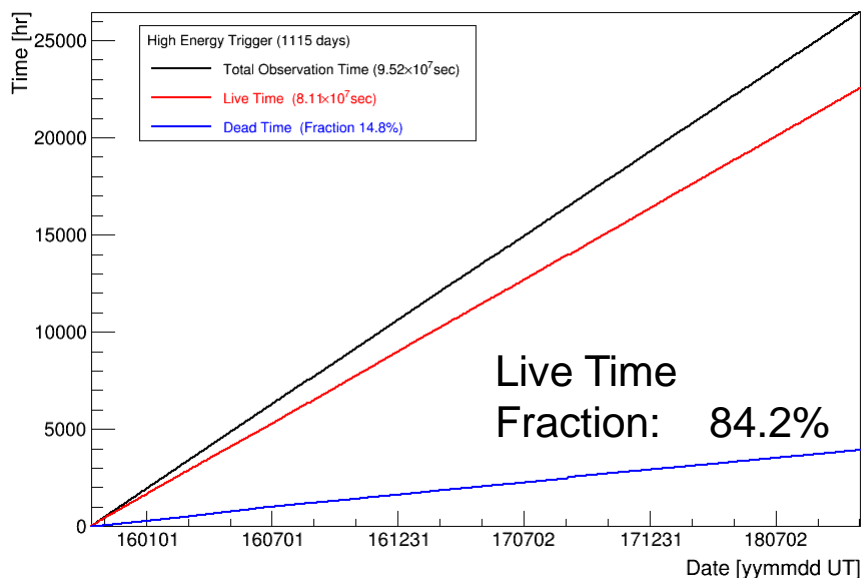




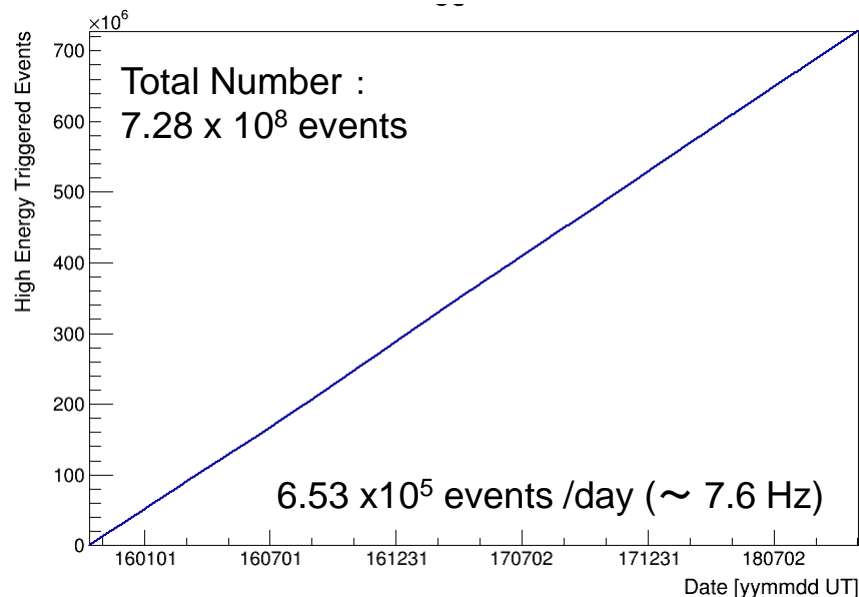
# Observation with High Energy Trigger (>10GeV)

Y.Asaoka, S.Ozawa, S.Torii et al. (CALET Collaboration), Astropart. Phys. 100 (2018) 29.

## Accumulated observation time (live, dead)



## Accumulated triggered event number



Observation by High Energy Trigger for 1115 days : Oct.13, 2015 – Oct. 31, 2018

- The exposure,  $SQT$ , has reached to  $\sim 97.6 \text{ m}^2 \text{ sr day}$  for electron observations by continuous and stable operations.
- Total number of triggered events is  $\sim 730$  million with a live time fraction of 84.2 %.



# All-Electron ( $e^+e^-$ )

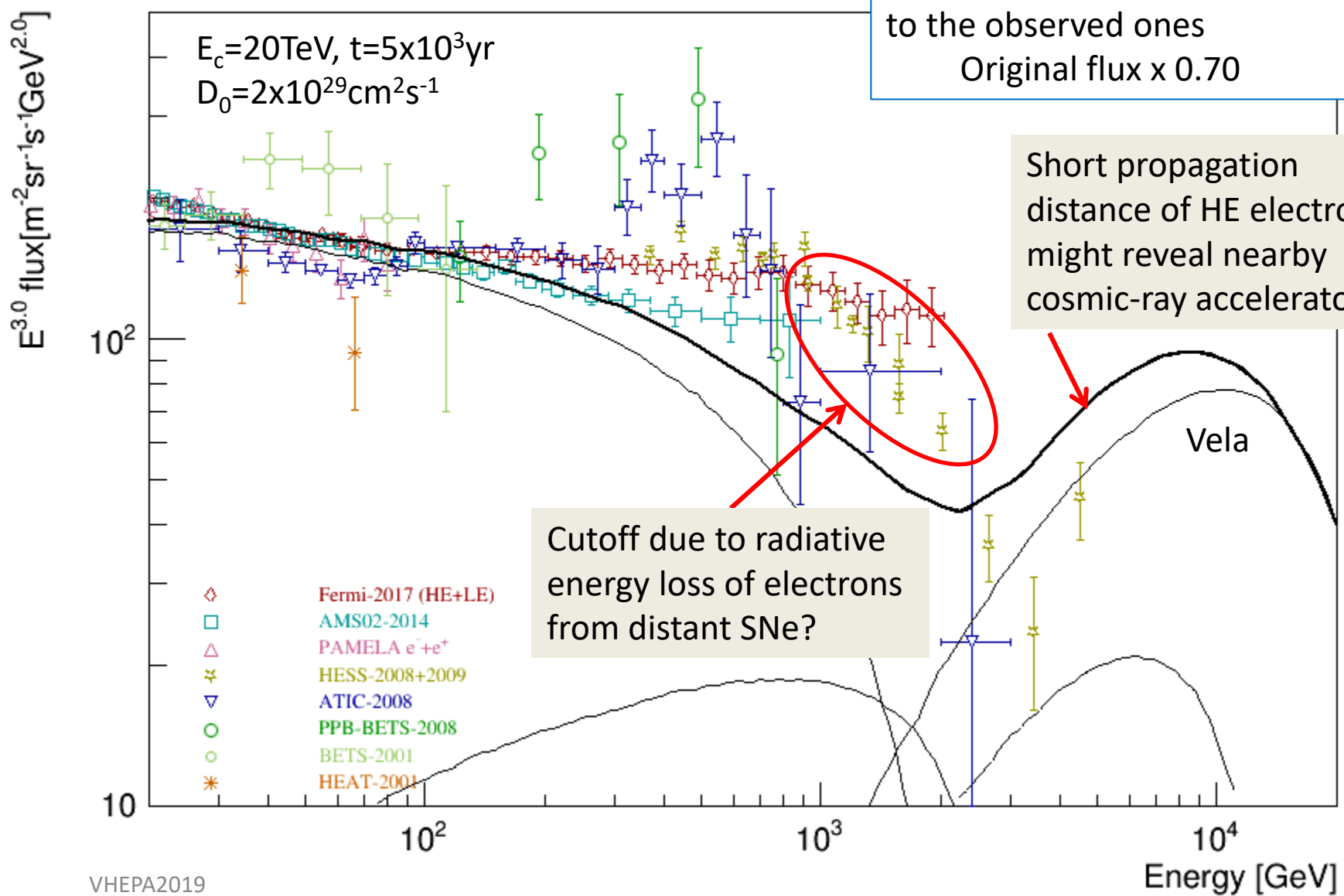
O.Adriani et al. (CALET collaboration), Phys. Rev. Lett. 119 (2017) 181101

O.Adriani et al. (CALET collaboration), Phys. Rev. Lett. 120 (2018) 261102

# Cosmic-Ray All-Electron Spectrum ( $e^+ + e^-$ )

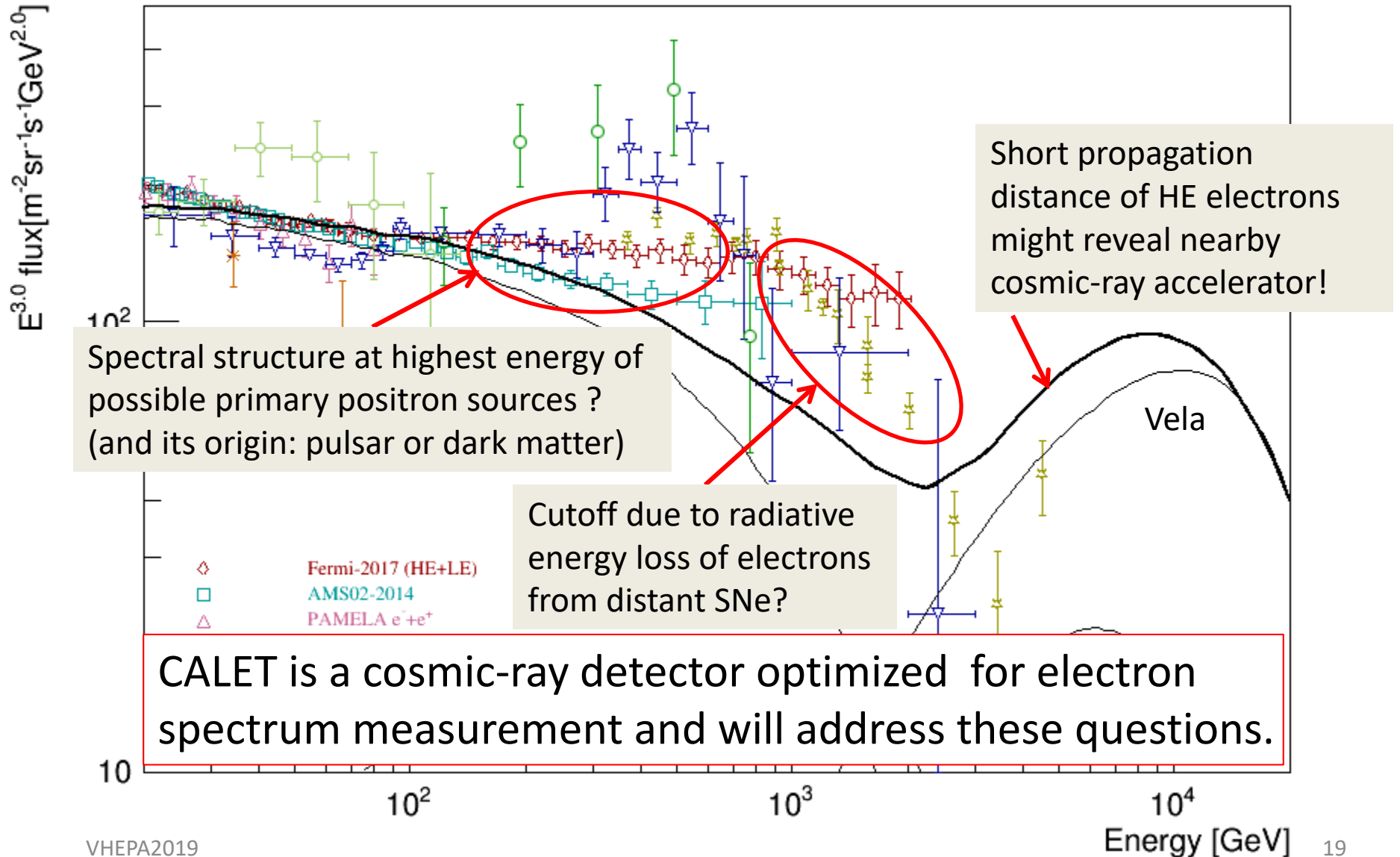
Kobayashi et al. ApJ 2004

Calculated results normalized to the observed ones  
Original flux x 0.70



# Cosmic-Ray All-Electron Spectrum ( $e^+ + e^-$ )

Possible fine structures in all-electron (electron + positron) spectrum

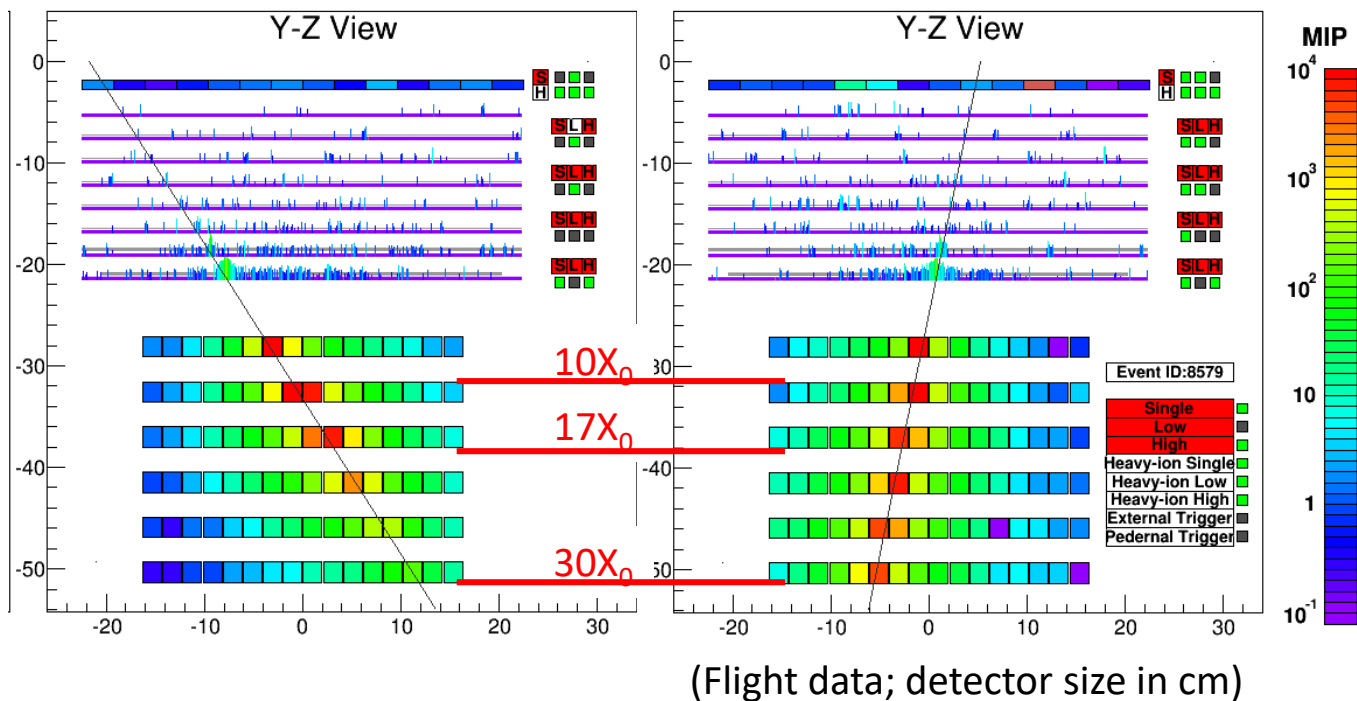




# All-Electron (electron + positron) Analysis

## 3TeV Electron Candidate

## Corresponding Proton Background



1. Reliable tracking  
well-developed  
shower core
2. Fine energy  
resolution  
full containment  
of TeV showers
3. High-efficiency  
electron ID  
30X<sub>0</sub> thickness,  
closely packed logs

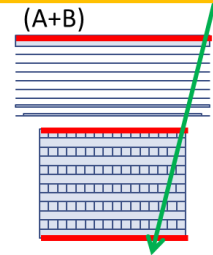
⇒ CALET is best suited for observation of **possible fine structures** in the all-electron spectrum up to the trans-TeV region.



# Event Selection

## Analyzed Flight Data:

- 627 days (October 13, 2015 to June 30, 2017)
- 55% of full CALET acceptance (Acceptance A+B;  $570\text{cm}^2\text{sr}$ )



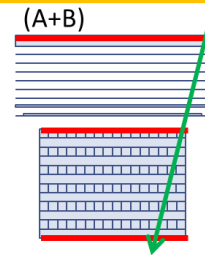
1. Offline Trigger
2. Acceptance Cut
3. Single Charge Selection
4. Track Quality Cut
5. Shower Development Consistency
6. Electron Identification
  1. Simple two parameter cut
  2. Multivariate Analysis using Boosted Decision Trees (BDT)



# Event Selection

## Analyzed Flight Data:

- 627 days (October 13, 2015 to June 30, 2017)
- 55% of full CALET acceptance (Acceptance A+B;  $570\text{cm}^2\text{sr}$ )



1. Offline Trigger
2. Acceptance Cut
3. Single Charge Selection
4. Track Quality Cut
5. Shower Development Consistency
6. Electron Identification
  1. Simple two parameter cut
  2. Multivariate Analysis using Boosted Decision Trees (BDT)

## Pre-selection:

- Select events with successful reconstructions
- Rejecting heavier particles
- Equivalent sample between flight and MC data



# Electron Identification

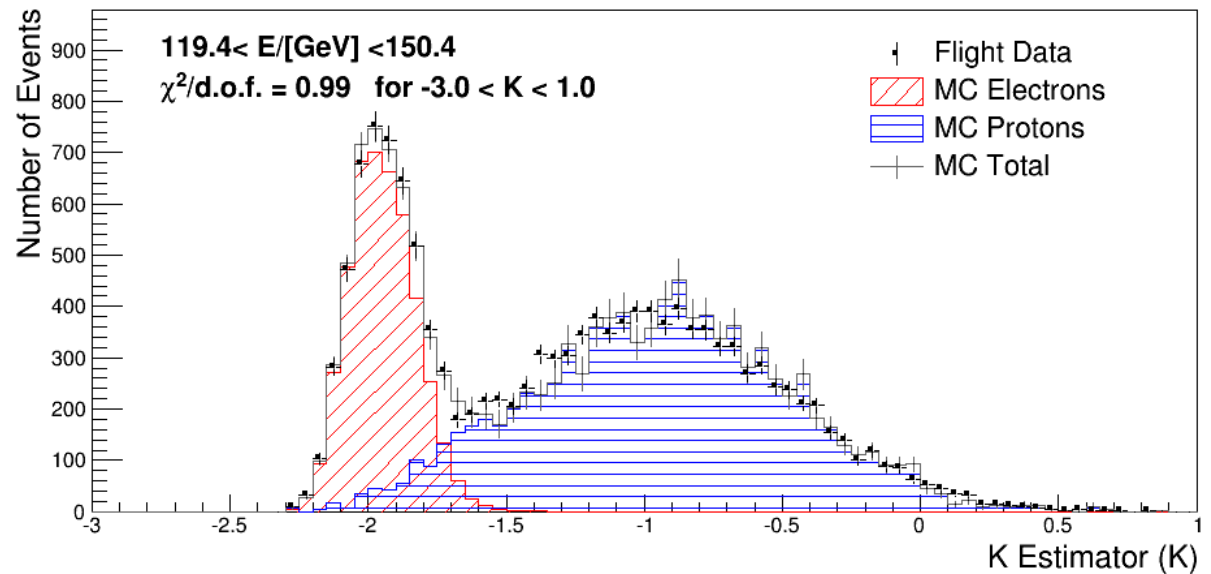
## Simple Two Parameter Cut

$F_E$ : Energy fraction of the bottom layer sum to the whole energy deposit sum in TASC

$R_E$ : Lateral spread of energy deposit in TASC-X1

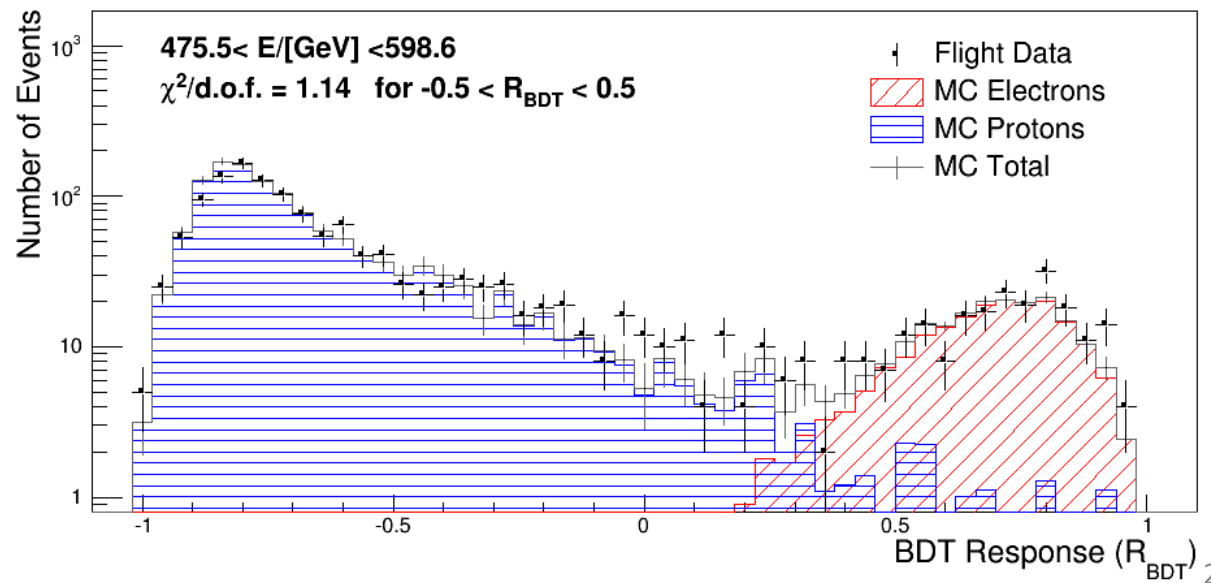
Separation Parameter  $K$  is defined as follows:

$$K = \log_{10}(F_E) + 0.5 R_E \text{ (/cm)}$$



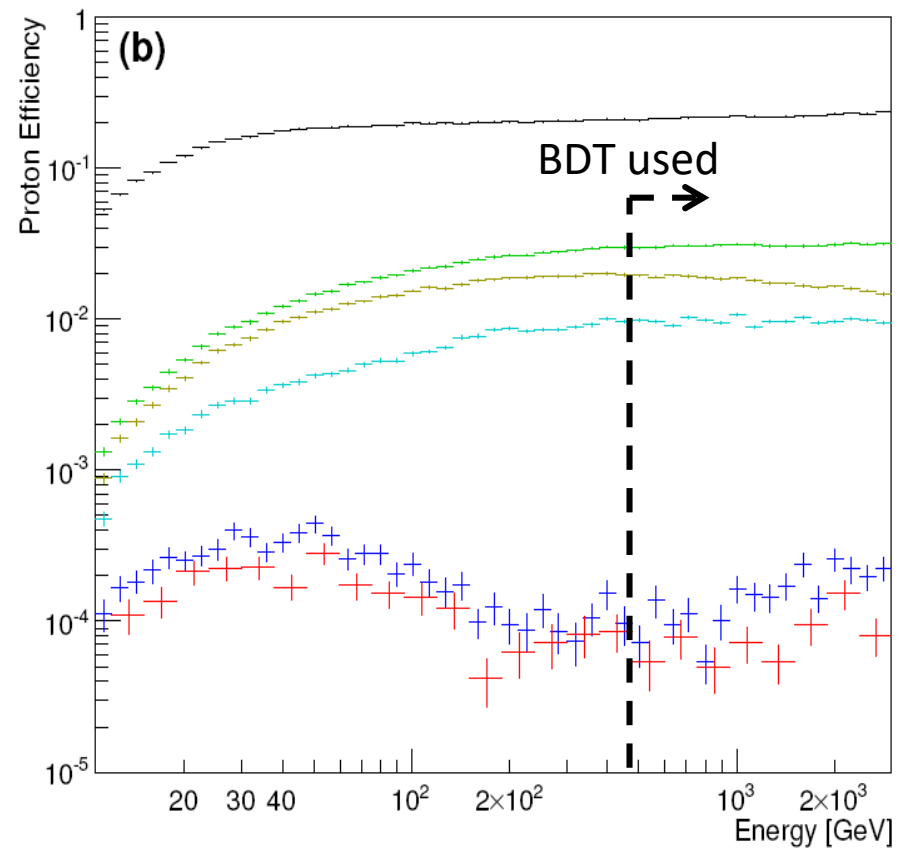
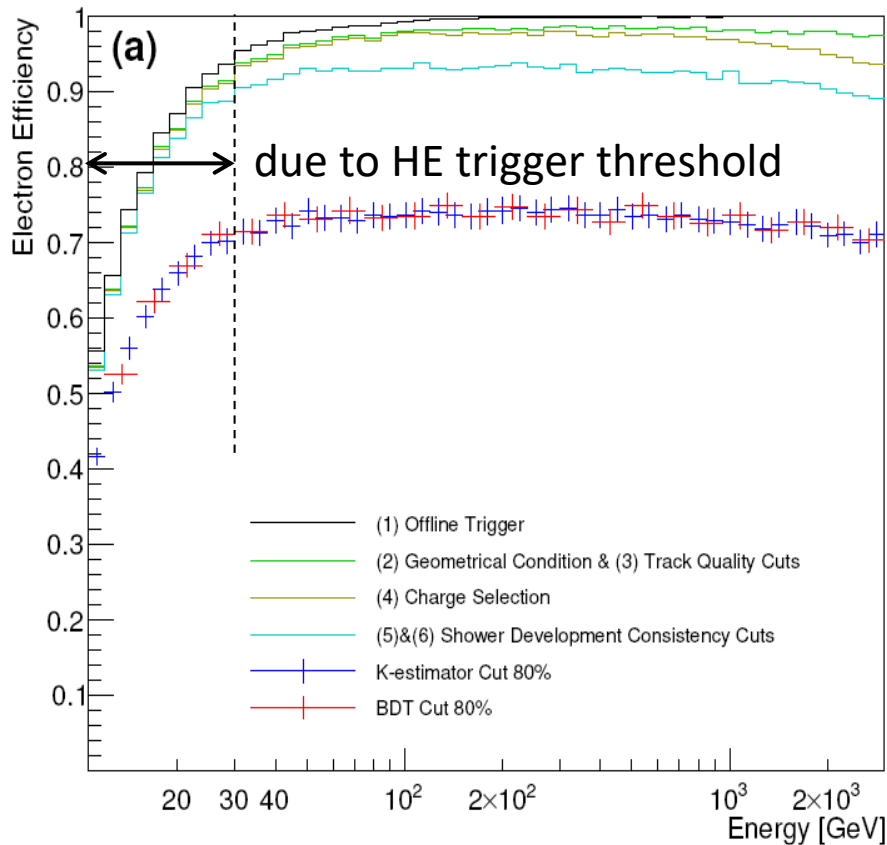
## Boosted Decision Trees

In addition to the two parameters making up  $K$ , TASC and IMC shower profile fits are used as discriminating variables.





# Electron Efficiency and Proton Rejection

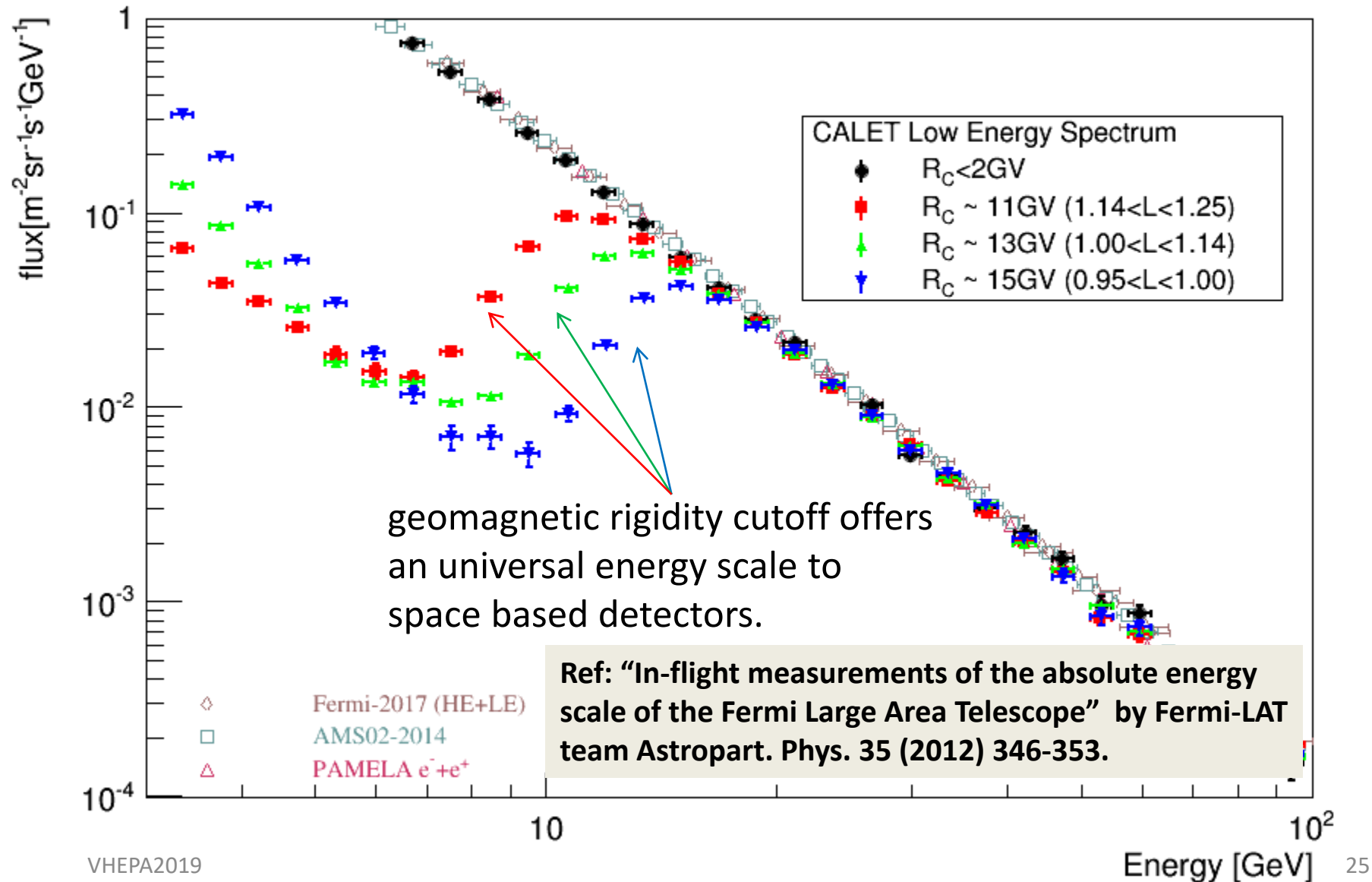


- Constant and high efficiency is the key point in our analysis.
- Simple two parameter (BDT) cut is used in the energy region  $E < 475 \text{ GeV}$  ( $E > 475 \text{ GeV}$ ) while the small difference in resultant spectrum between two methods are taken into account in the systematic uncertainty.
- Contamination is  $\sim 5\%$  up to 1 TeV, and  $< 15\%$  in the 1—3 TeV region.





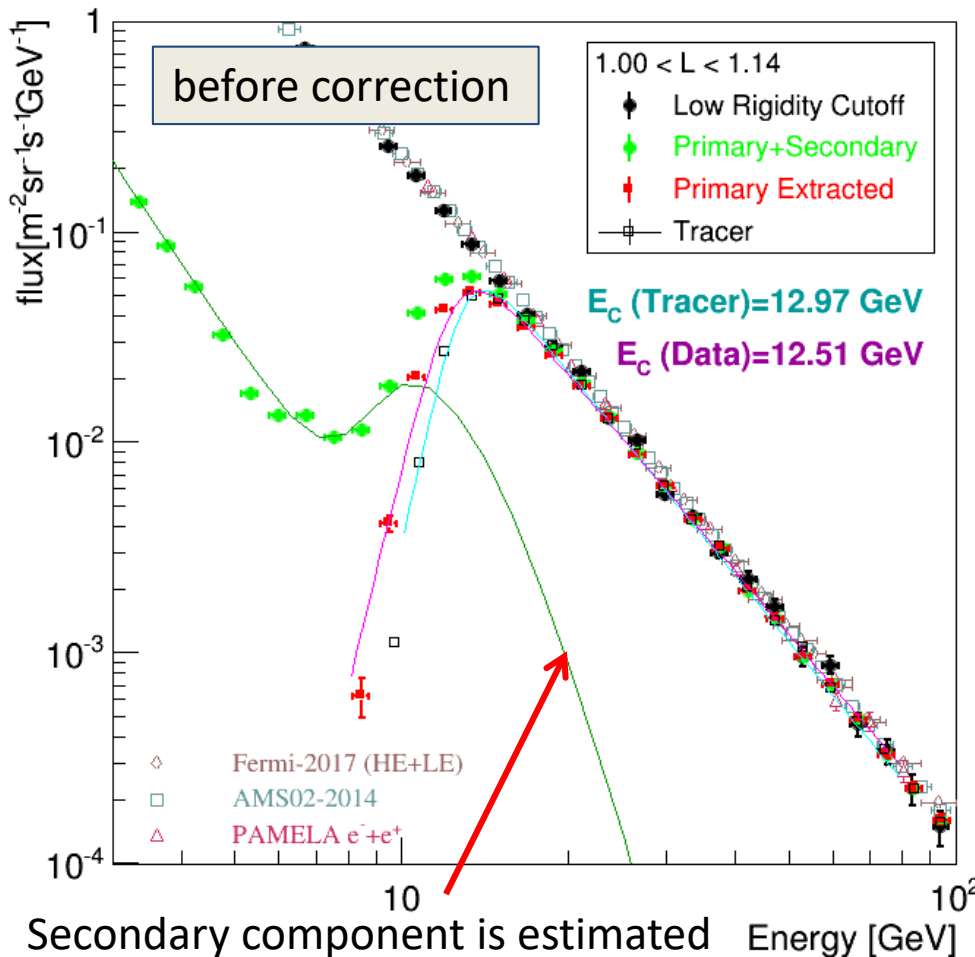
# Absolute Calibration of Energy Scale using Geomagnetic Rigidity Cutoff





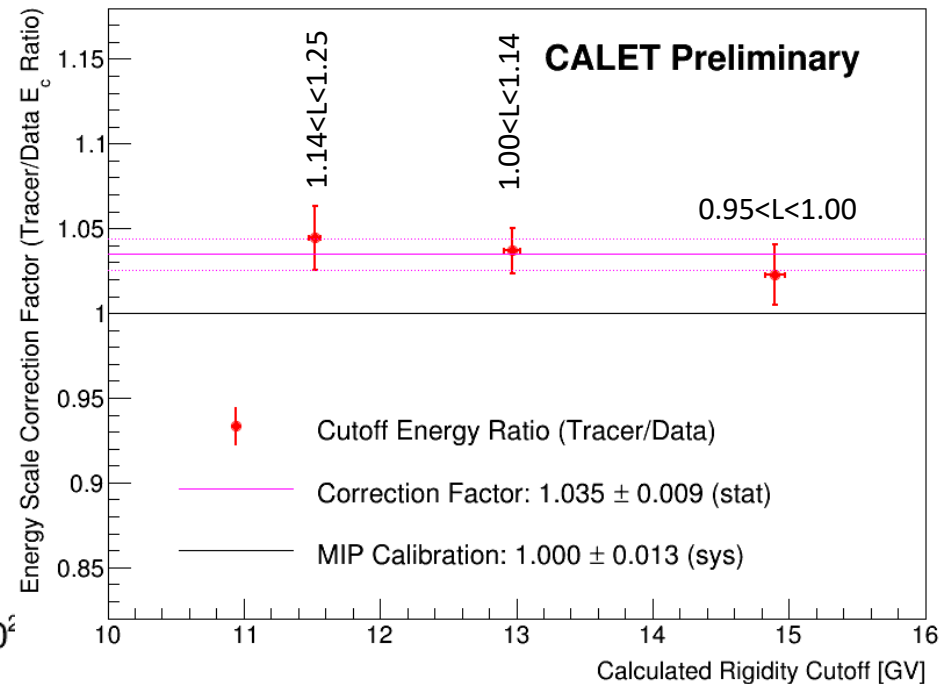
# Cutoff Rigidity Measurements and Comparison with Calculation

Measured cutoff rigidity is compared with calculated one (denoted as Tracer) which trace particle in earth's magnetic field (IGRF12).



Secondary component is estimated using azimuthal distributions

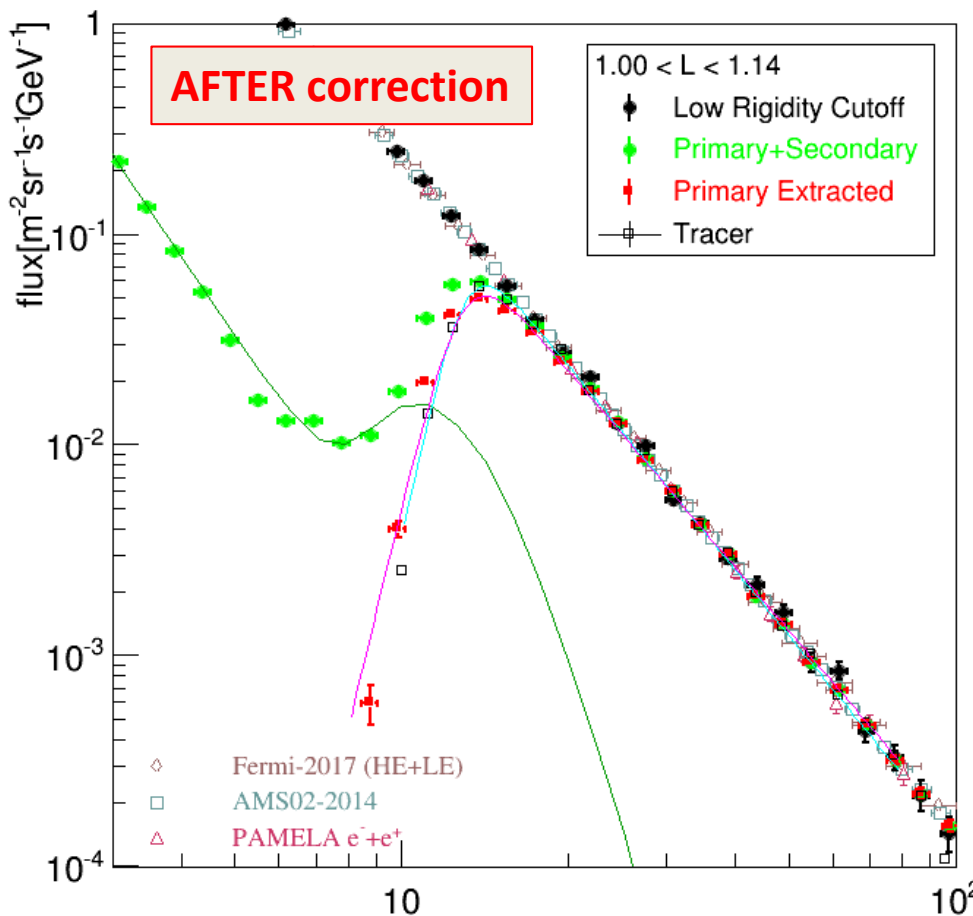
- Same analysis performed in 3 different rigidity cutoff regions.



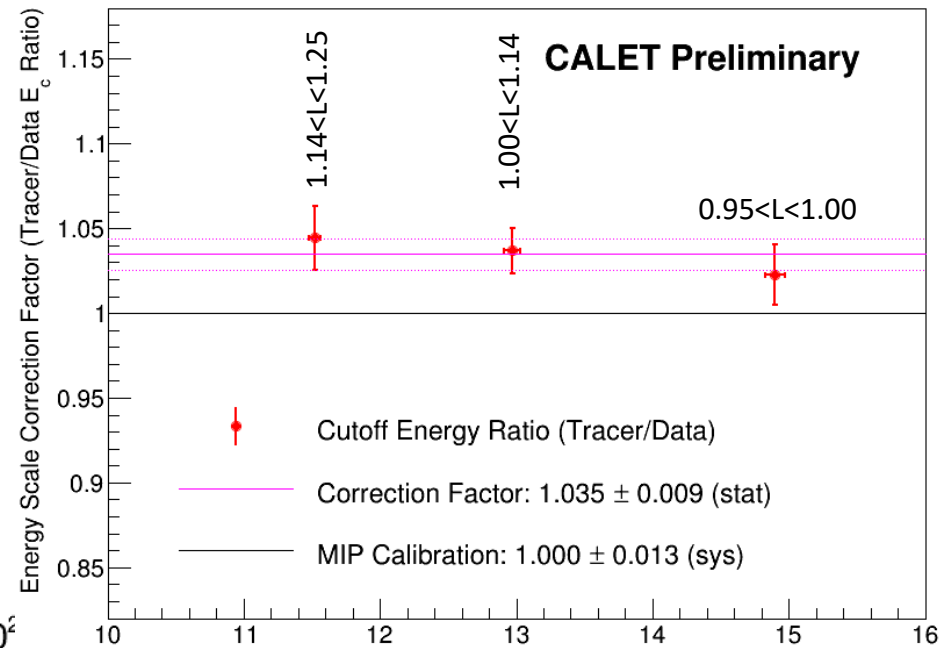


# Cutoff Rigidity Measurements and Comparison with Calculation

Measured cutoff rigidity is compared with calculated one (denoted as Tracer) which trace particle in earth's magnetic field (IGRF12).



- Same analysis performed in 3 different rigidity cutoff regions.  
⇒ Correction factor was found to be **1.035** compared to MIP calibration.

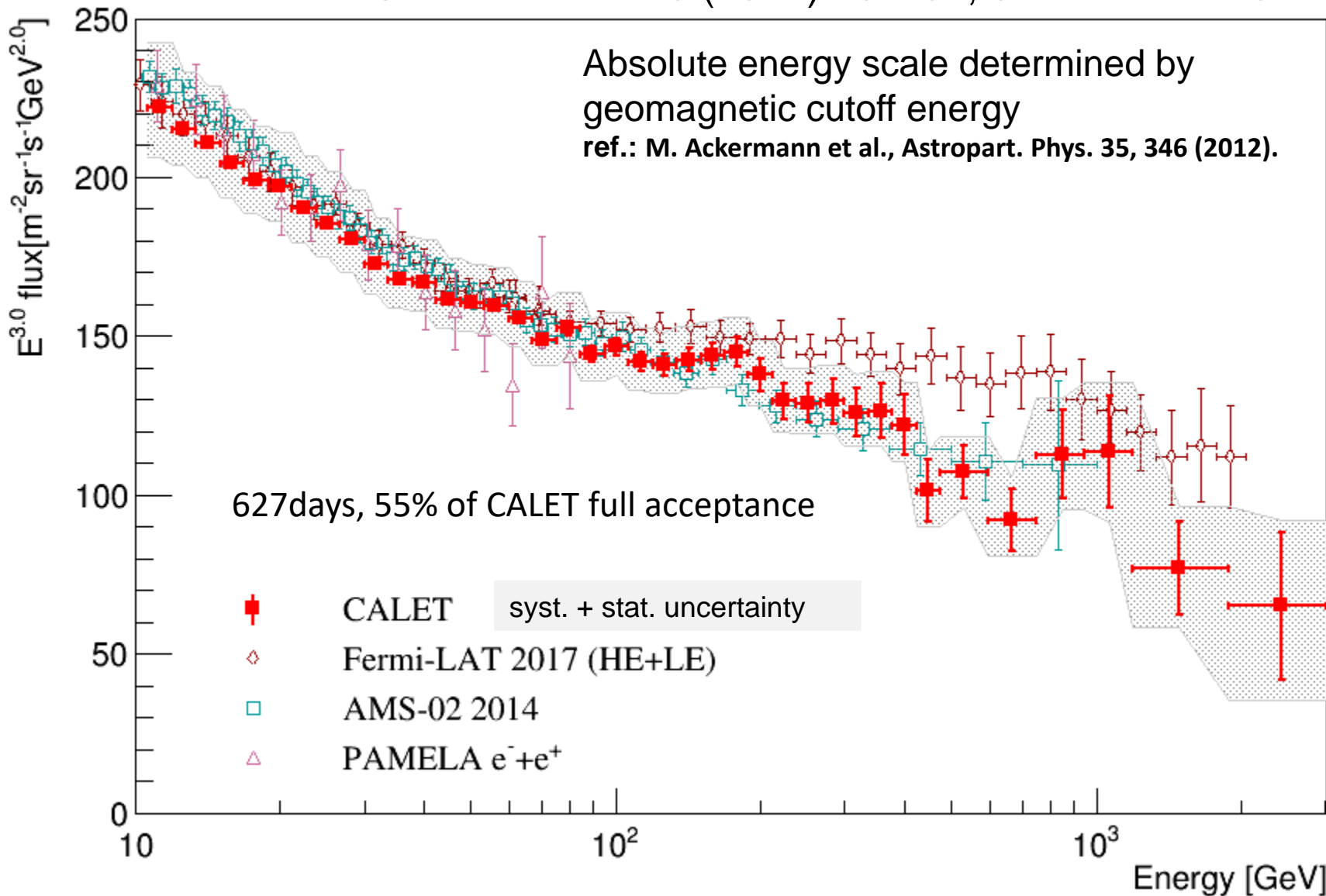


Since universal energy-scale calibration between different instruments is very important, we adopt the energy scale determined by rigidity cutoff to derive our spectrum.



# All-Electron Spectrum Measured with CALET from 10 GeV to 3 TeV

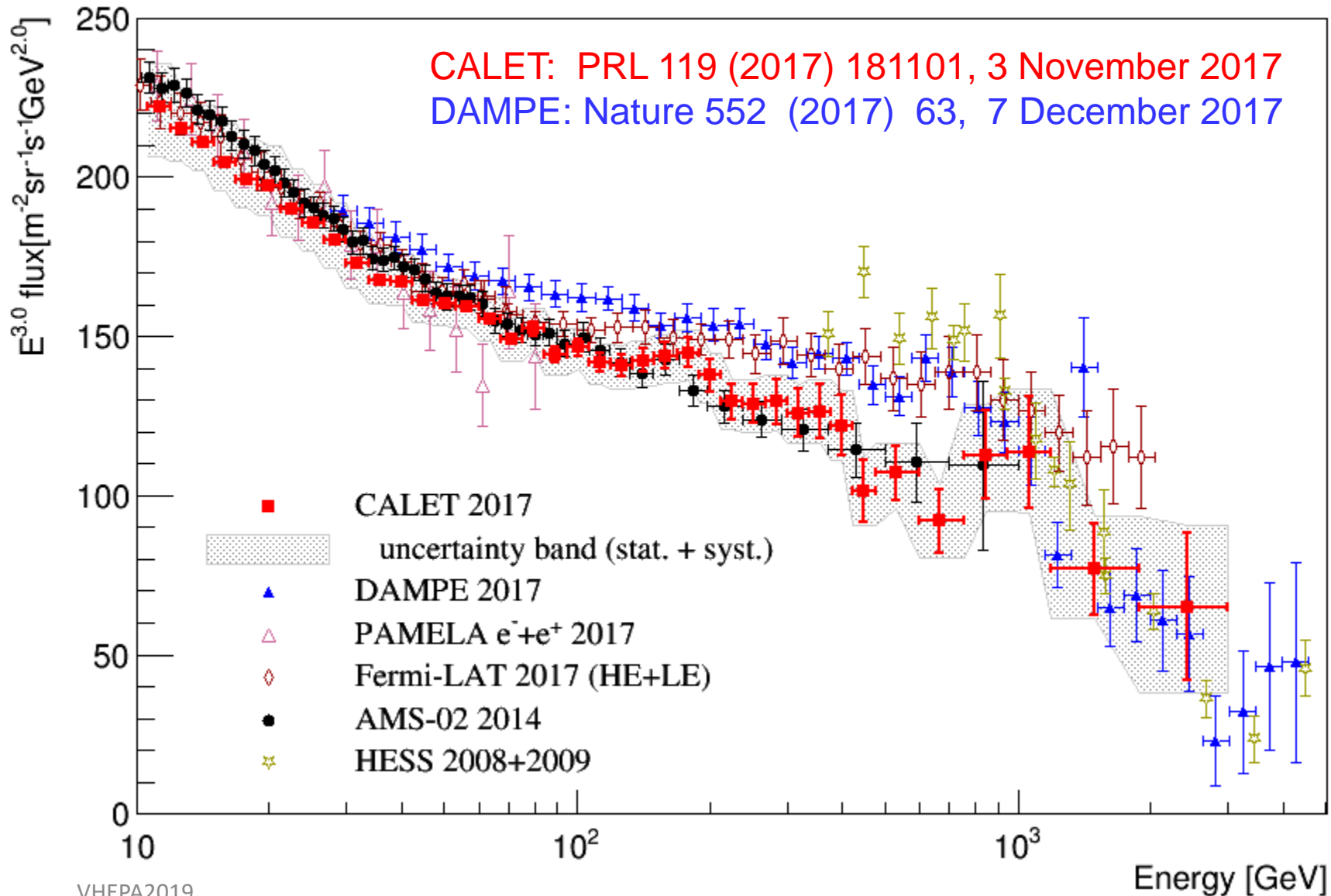
CALET: PRL 119 (2017) 181101, 3 November 2017





# All-Electron Spectrum Comparison w/ DAMPE

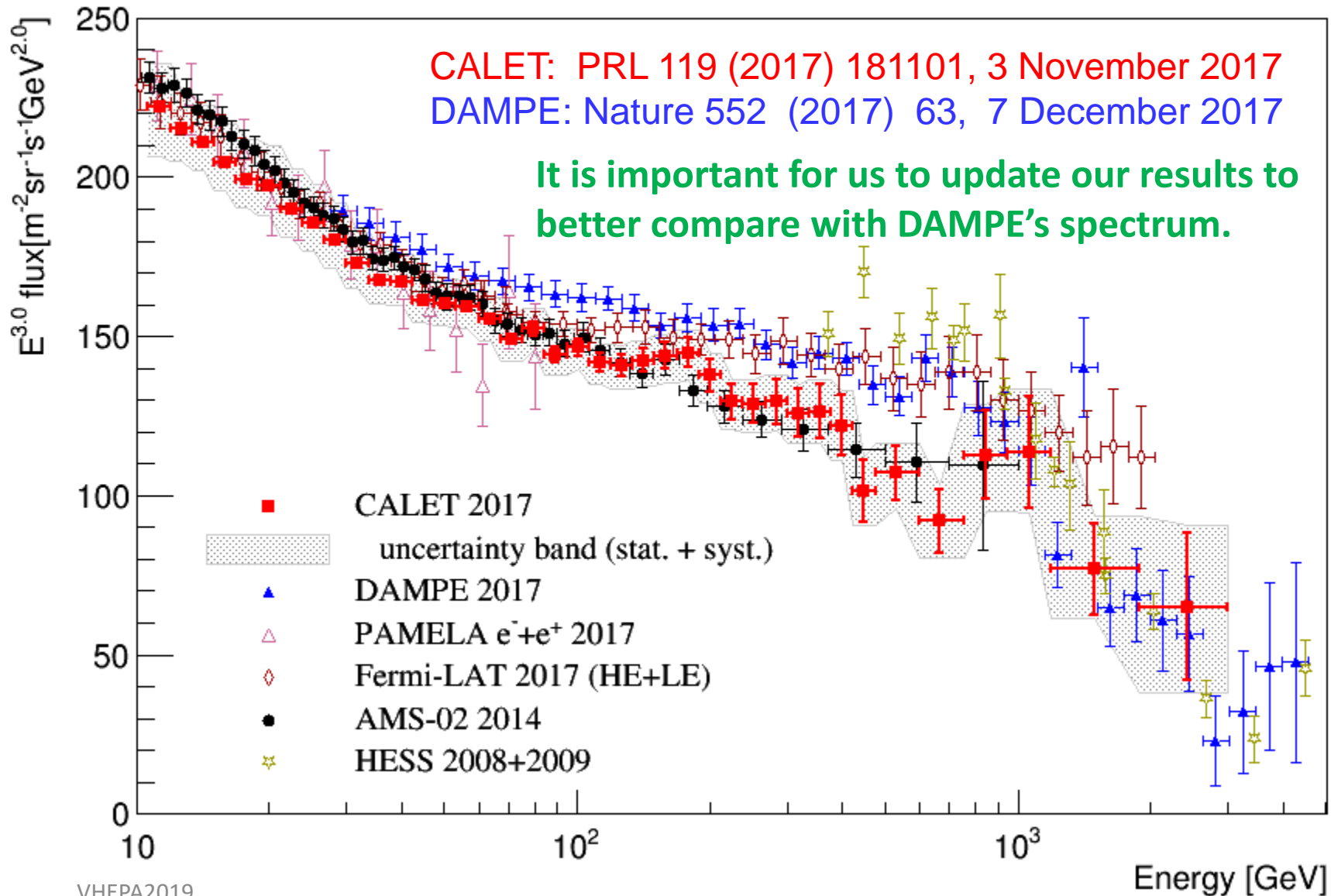
and other space based experiments





# All-Electron Spectrum Comparison w/ DAMPE

and other space based experiments

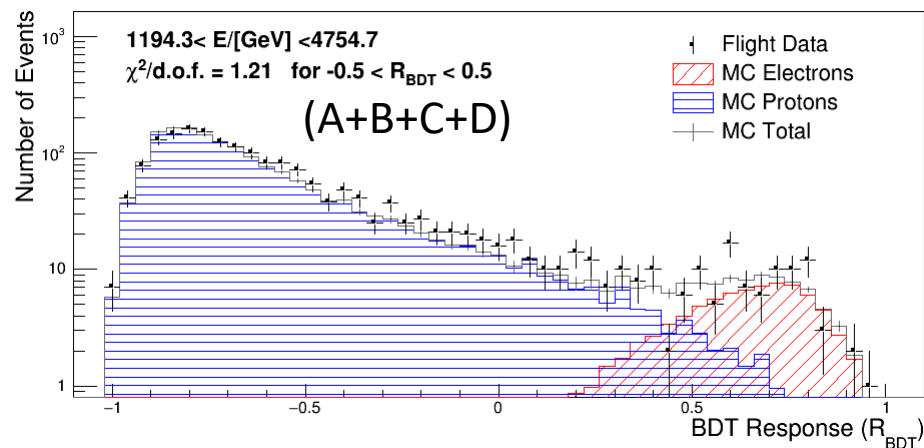
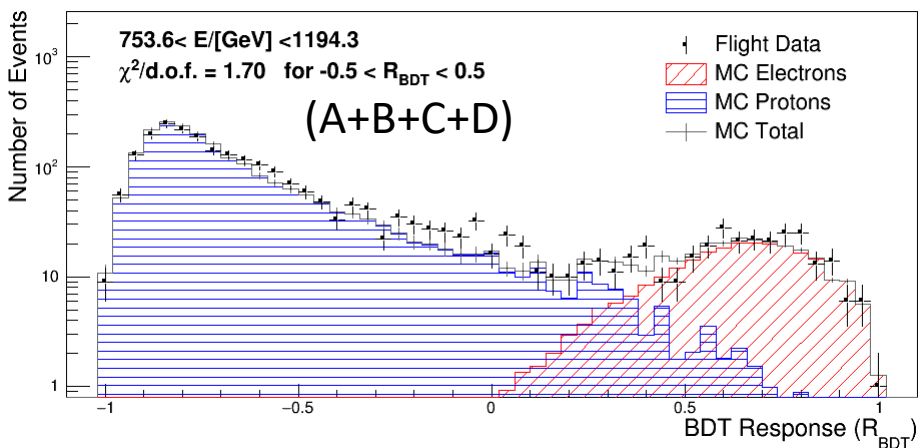
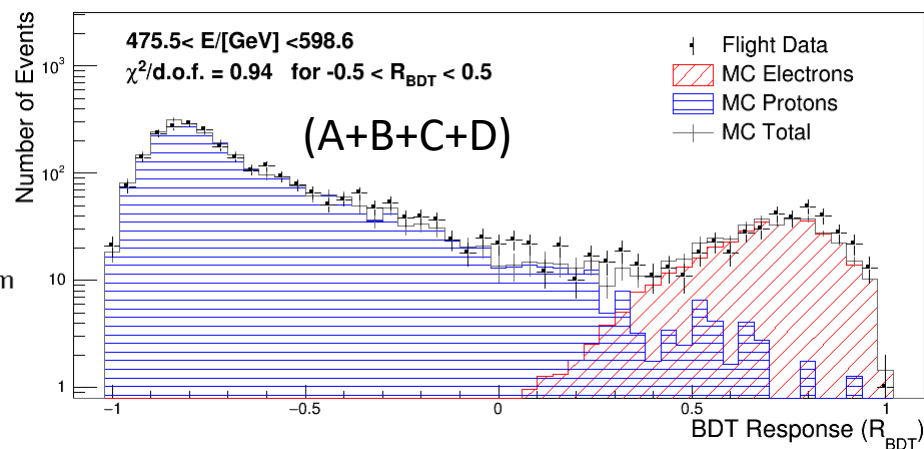
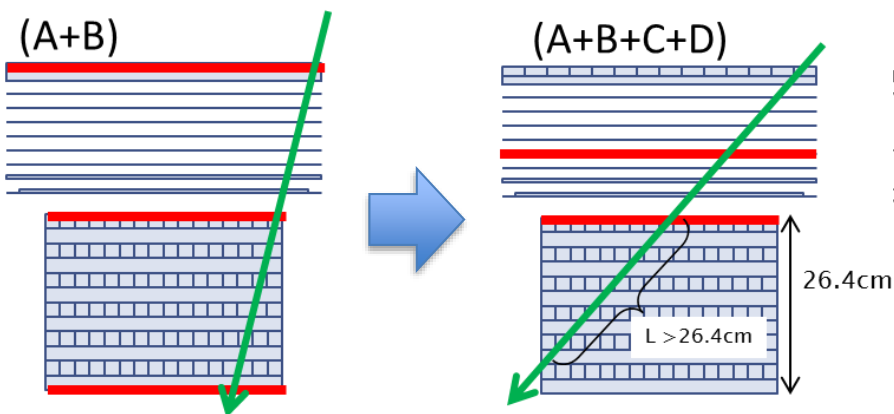




# Extending the Analysis to Full Acceptance

## Analyzed Flight Data:

- 780 days (October 13, 2015 to November 30, 2017)
- Full CALET acceptance at the high energy region** (Acceptance A+B+C+D; 1040cm<sup>2</sup>sr).  
In the low energy region fully contained events are used (A+B; 550cm<sup>2</sup>sr)





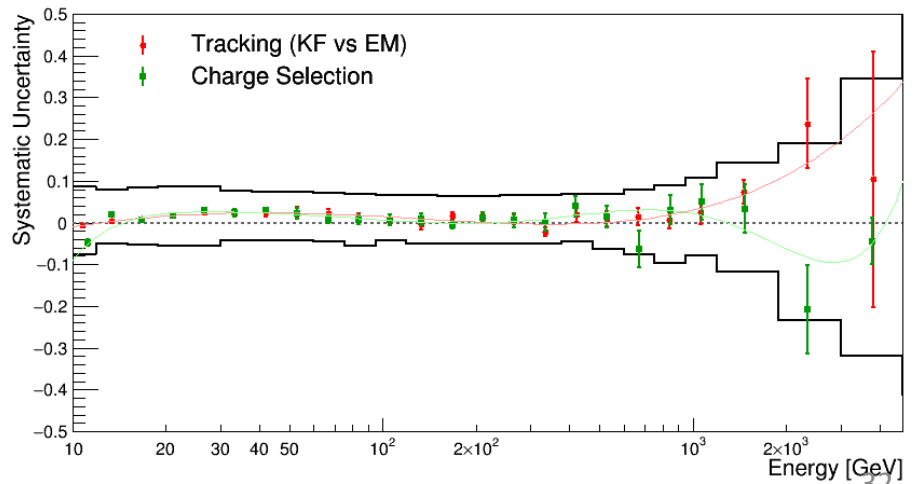
# Systematic Uncertainties

(other than energy scale uncertainty)

## Stability of resultant flux are analyzed by scanning parameter space

- Normalization:
  - Live time
  - Radiation environment
  - Long-term stability
  - Quality cuts
- Energy dependent:
  - 2 independent tracking
  - charge ID
  - electron ID (K-Cut vs BDT)
  - BDT stability (vs efficiency & training)
  - MC model (EPICS vs Geant4)

The energy scale uncertainty does not have energy dependence, because of the full containment of the EM showers well into the TeV region. Errors due to calibration of lower gain ranges are found to be negligible.







# Systematic Uncertainties

(other than energy scale uncertainty)

**Stability of resultant flux are analyzed by scanning parameter space**

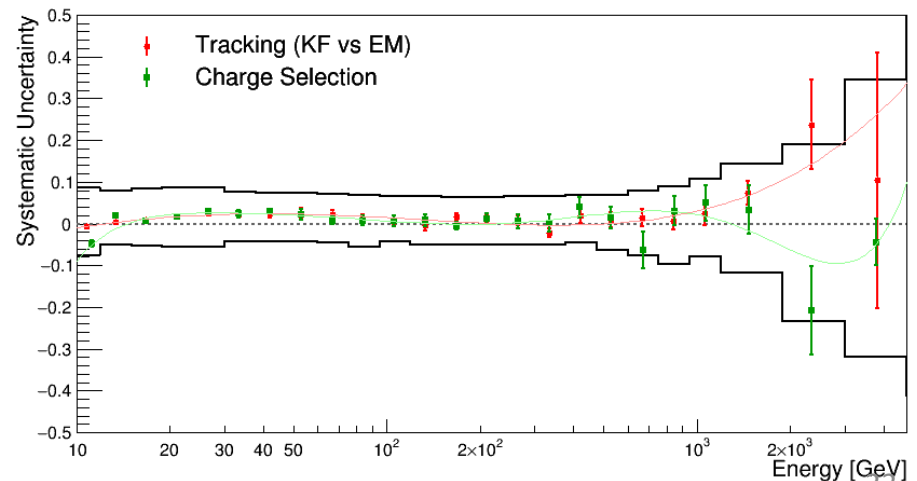
- Normalization:

- Live time
- Radiation environment
- Long-term stability
- Quality cuts

- Energy dependent:

- 2 independent tracking
- charge ID
- electron ID (K-Cut vs BDT)
- BDT stability (vs efficiency & training)
- MC model (EPICS vs Geant4)

1. Divided into 4 sub-periods (195days each)
2. spectrum in each sub-period is compared with the one from the whole period.
3. standard deviation of the relative difference distribution is taken as systematic uncertainty (1.4%)





# Systematic Uncertainties

(other than energy scale uncertainty)

**Stability of resultant flux are analyzed by scanning parameter space**

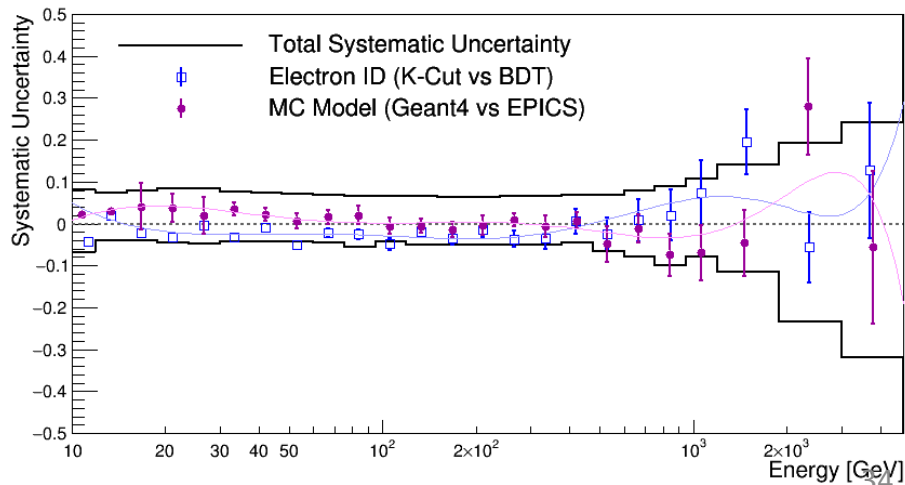
- Normalization:

- Live time
- Radiation environment
- Long-term stability
- Quality cuts

- Energy dependent:

- 2 independent tracking
- charge ID
- electron ID (K-Cut vs BDT)
- BDT stability (vs efficiency & training)
- MC model (EPICS vs Geant4)

1. Divided into 4 sub-periods (195days each)
2. spectrum in each sub-period is compared with the one from the whole period.
3. standard deviation of the relative difference distribution is taken as systematic uncertainty (1.4%)





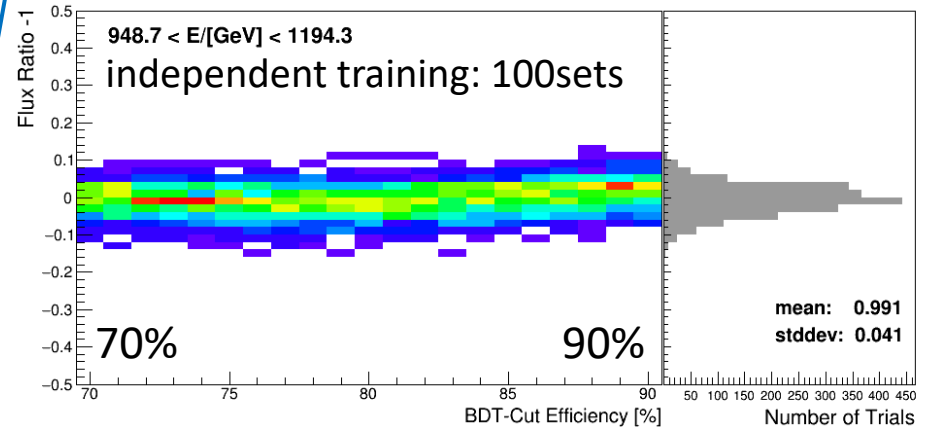
# Systematic Uncertainties

(other than energy scale uncertainty)

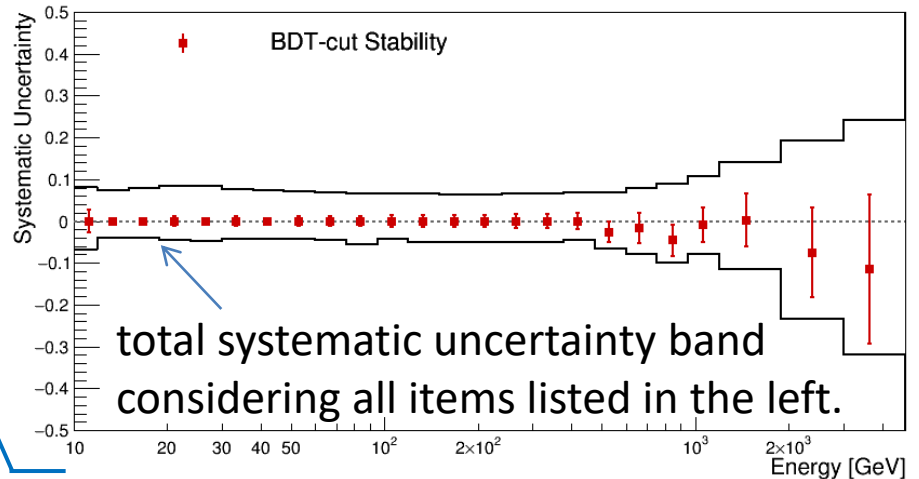
**Stability of resultant flux are analyzed by scanning parameter space**

- Normalization:
  - Live time
  - Radiation environment
  - Long-term stability
  - Quality cuts
- Energy dependent:
  - 2 independent tracking
  - charge ID
  - electron ID (K-Cut vs BDT)
  - **BDT stability** (vs efficiency & training)
  - MC model (EPICS vs Geant4)

Flux Ratio vs Efficiency for BDT @ 1TeV



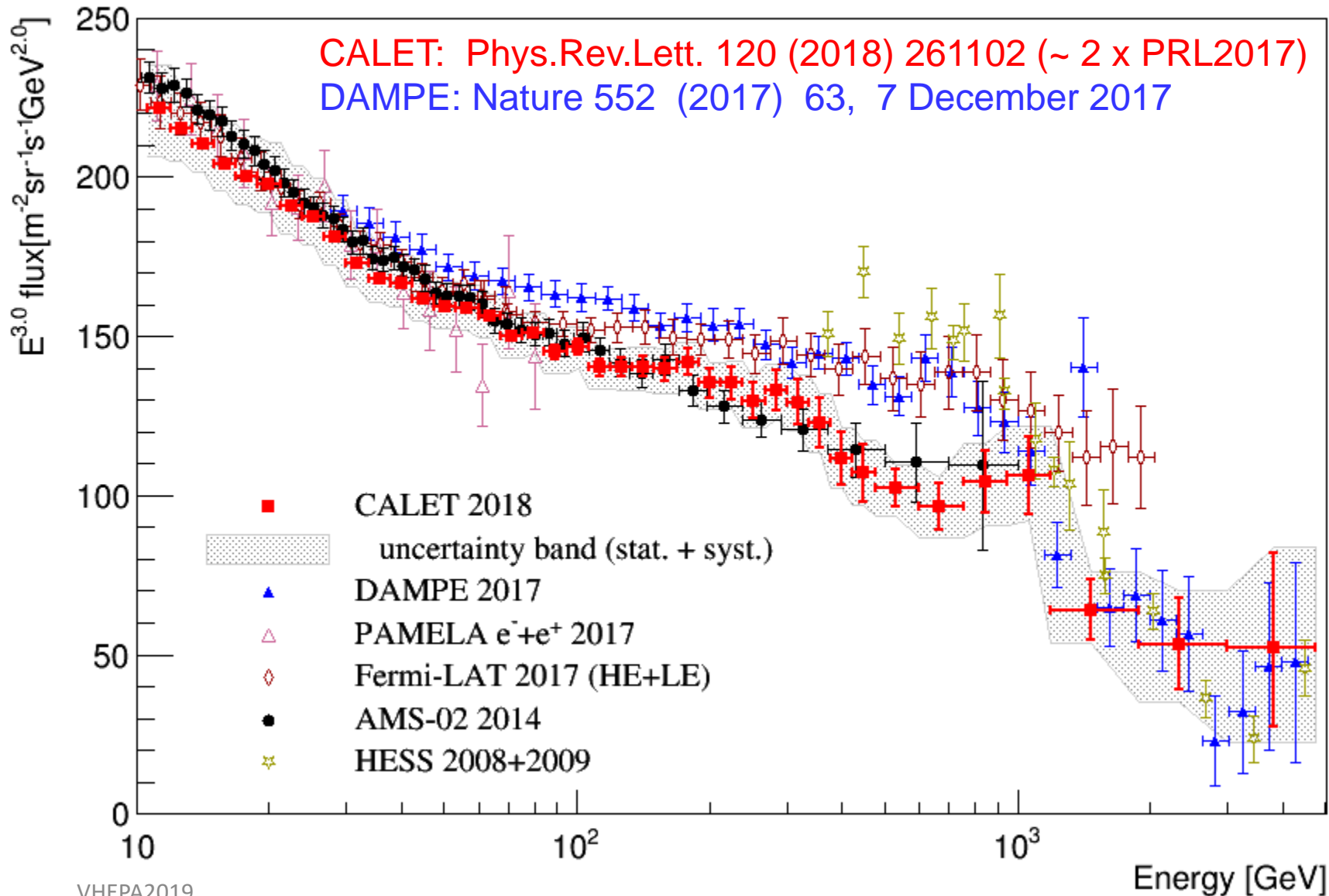
Energy Dependence of BDT stability





# Extended Measurement by CALET

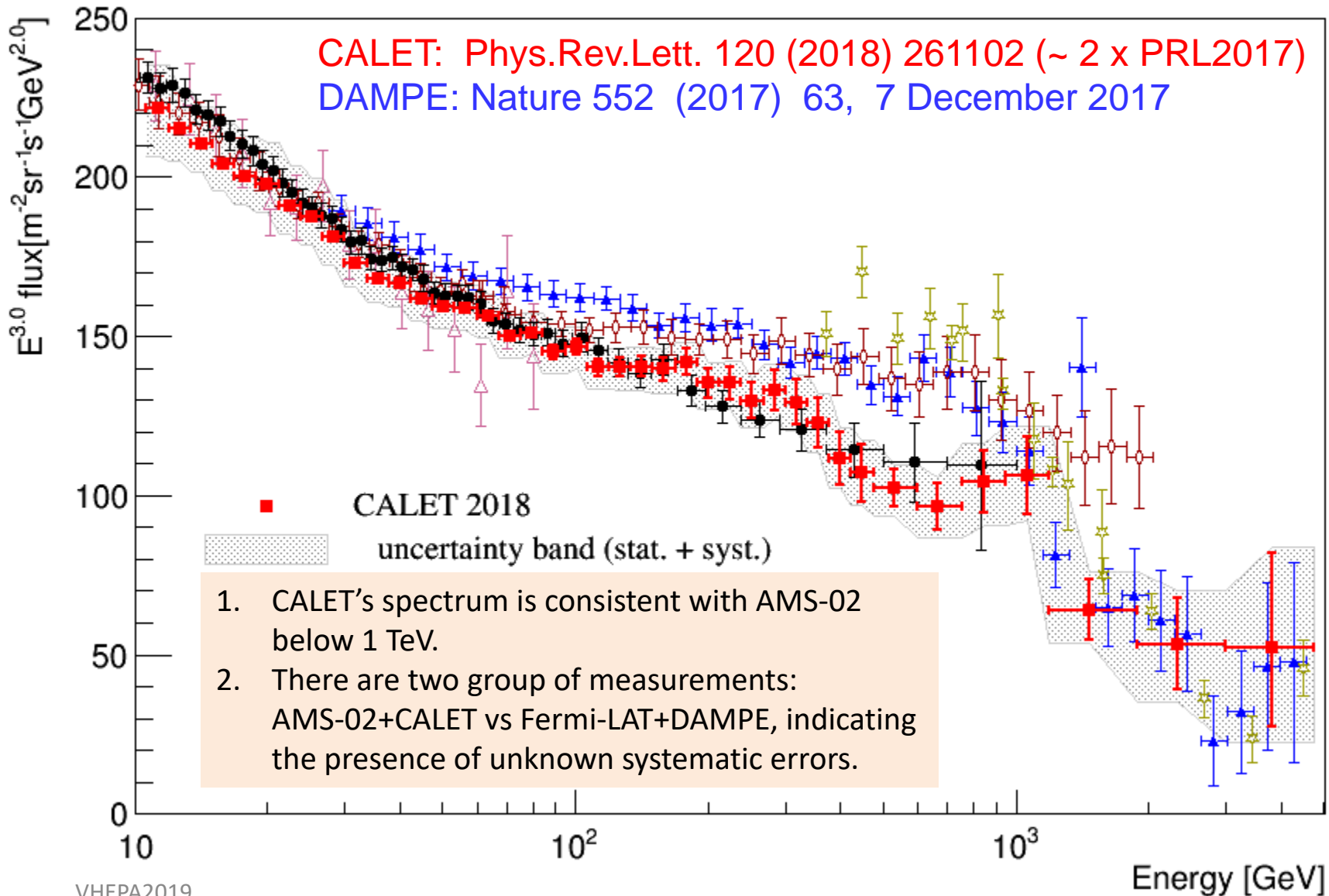
Approximately doubled statistics above 500GeV by using full acceptance of CALET





# Extended Measurement by CALET

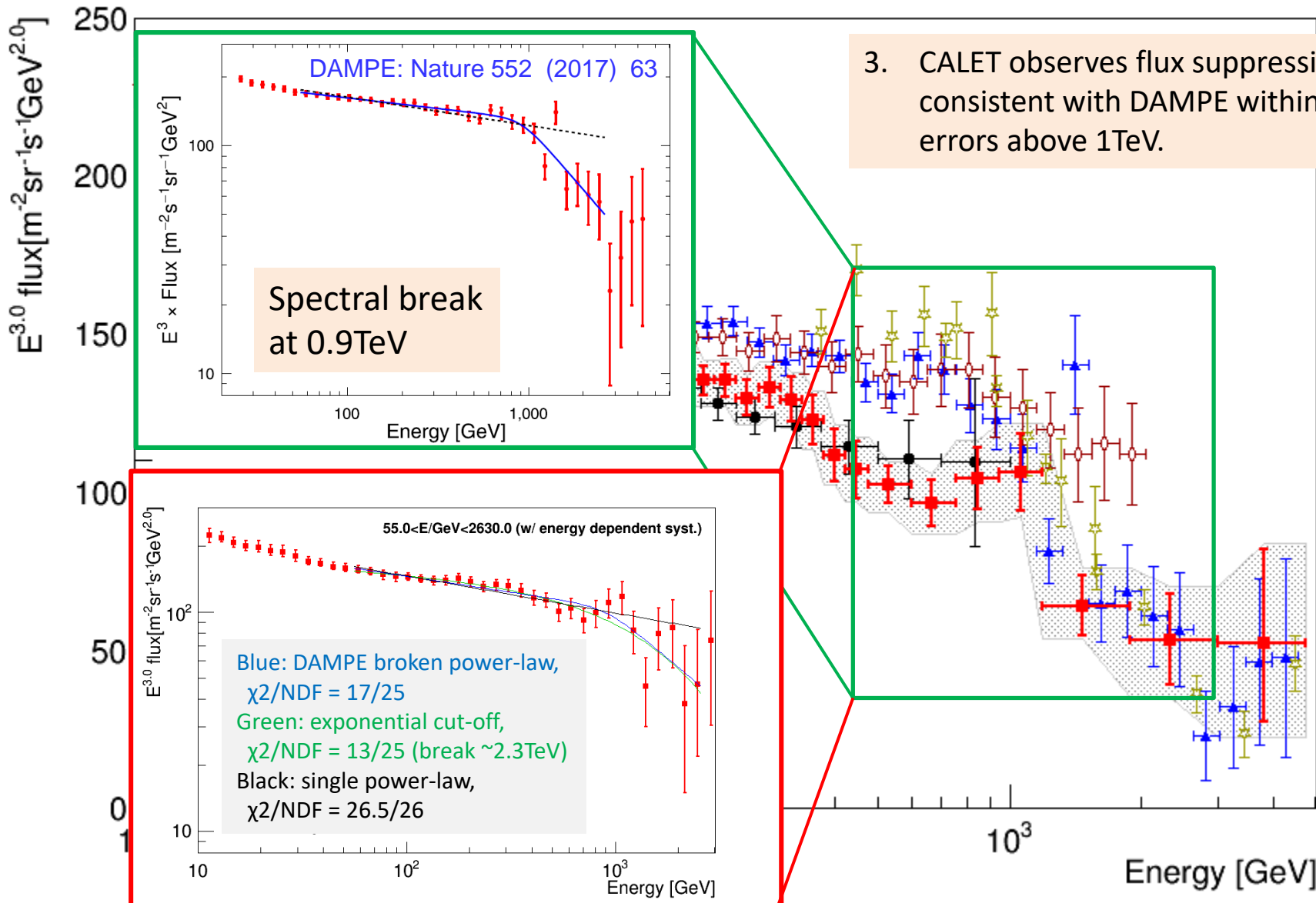
Approximately doubled statistics above 500GeV by using full acceptance of CALET





# Extended Measurement by CALET

Approximately doubled statistics above 500GeV by using full acceptance of CALET



3. CALET observes flux suppression consistent with DAMPE within errors above 1TeV.

Spectral break at 0.9TeV

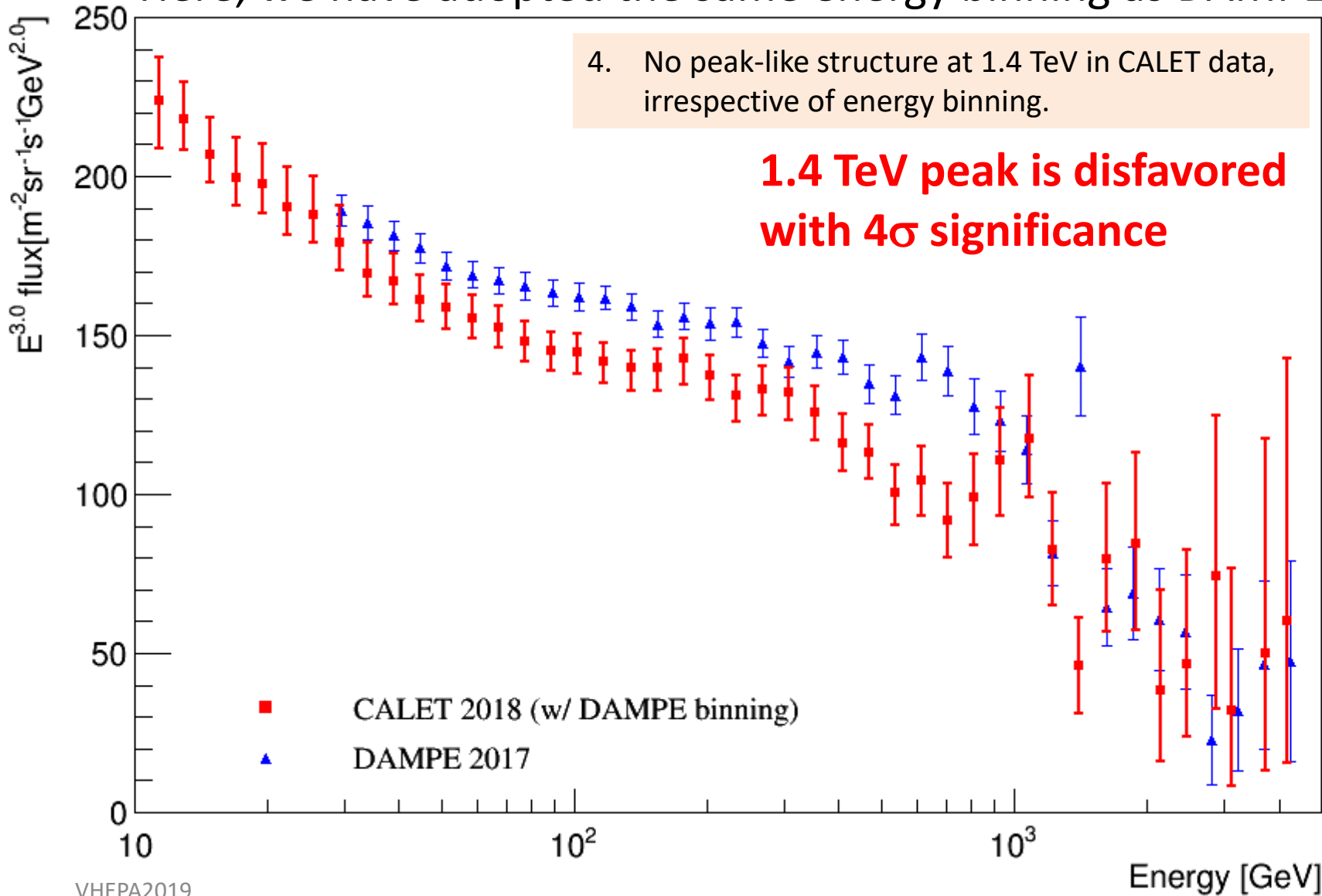
55.0 < E/GeV < 2630.0 (w/ energy dependent syst.)

Blue: DAMPE broken power-law,  $\chi^2/NDF = 17/25$   
Green: exponential cut-off,  $\chi^2/NDF = 13/25$  (break  $\sim 2.3\text{TeV}$ )  
Black: single power-law,  $\chi^2/NDF = 26.5/26$



# Comparison with DAMPE's result

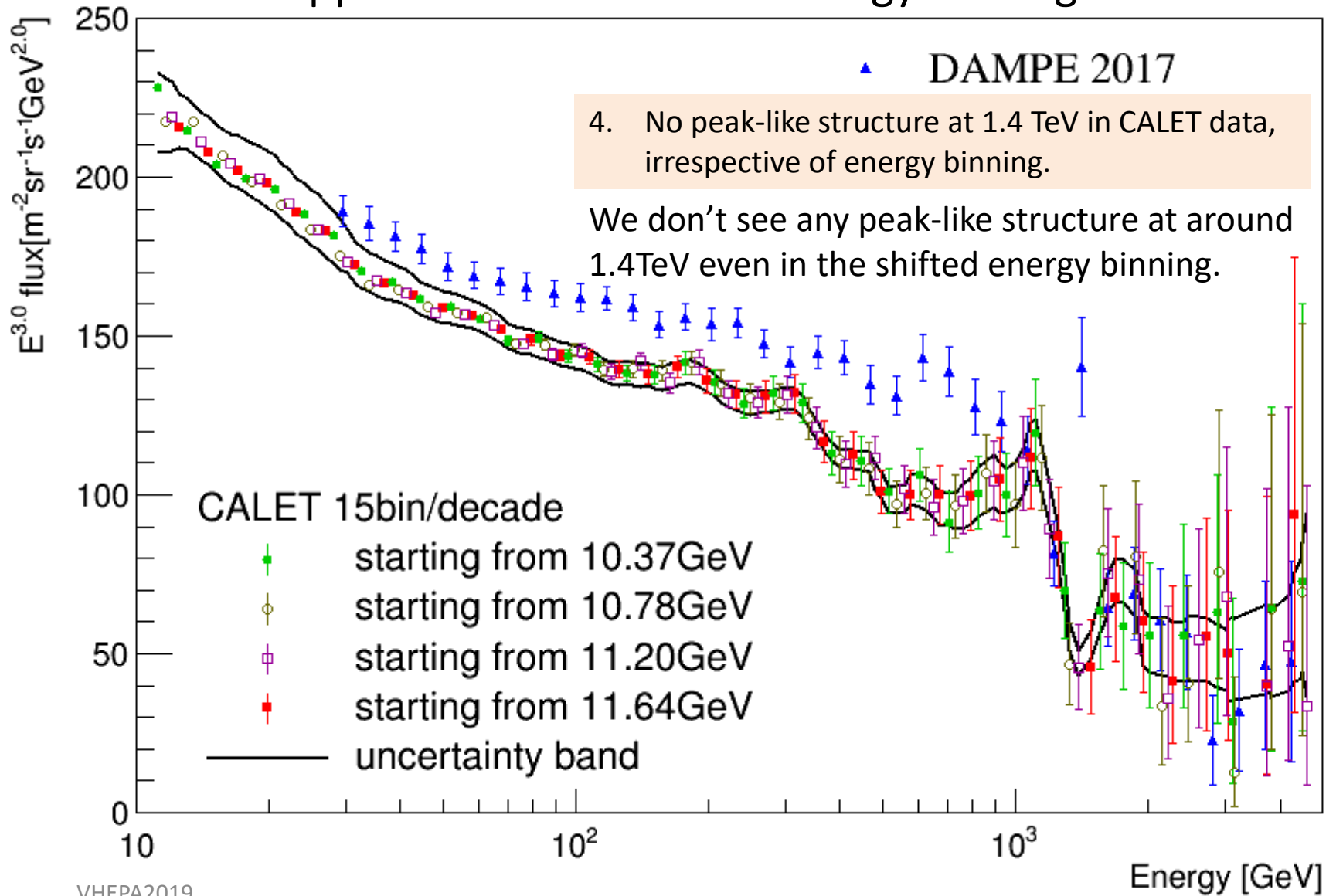
Here, we have adopted the same energy binning as DAMPE.





# Comparison with DAMPE's result

What happens if we shifted our energy binning...

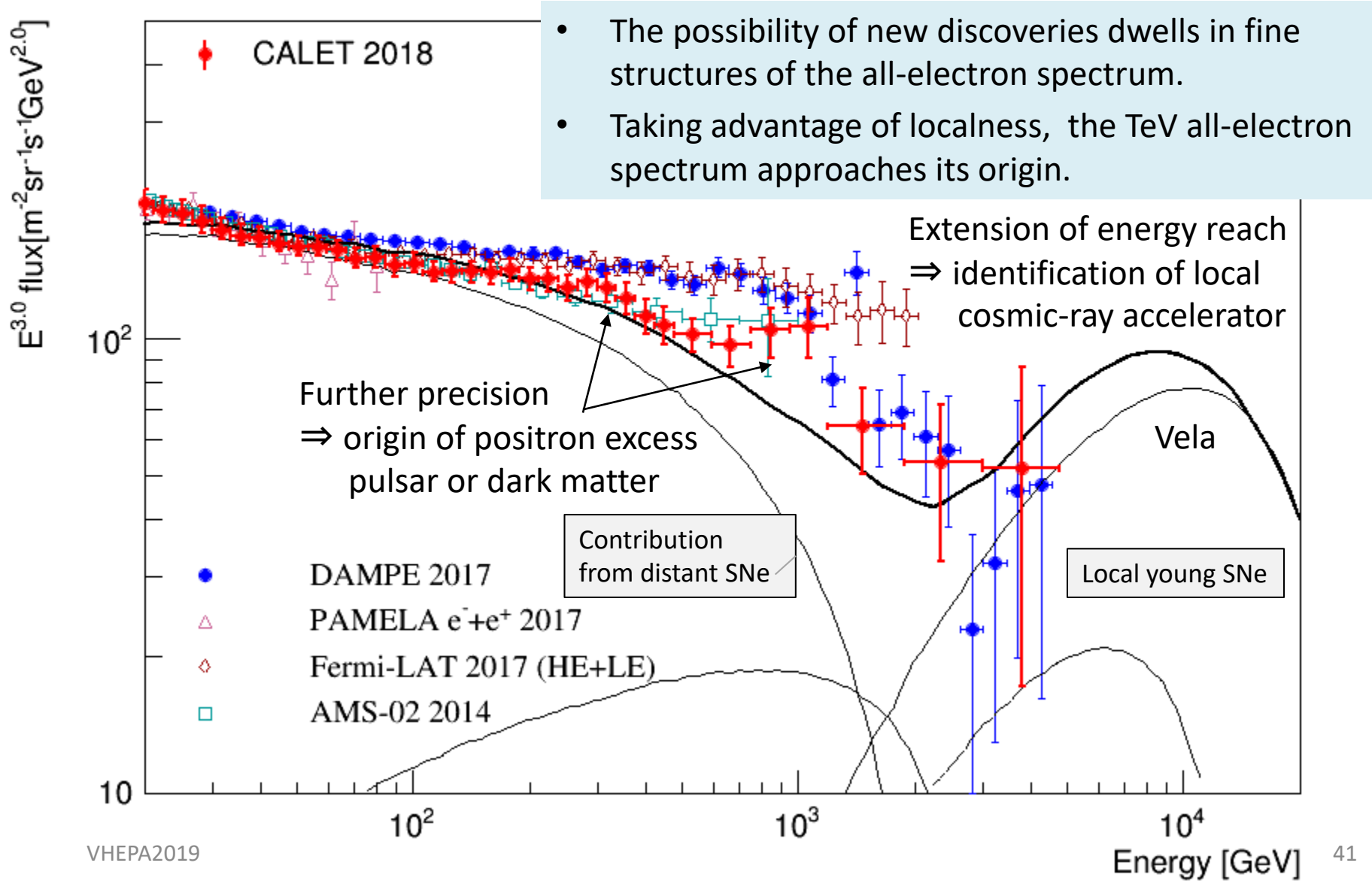






# Prospects for CALET All-Electron Spectrum

Five years or more observations  $\Rightarrow$  3 times more statistics, reduction of systematic errors



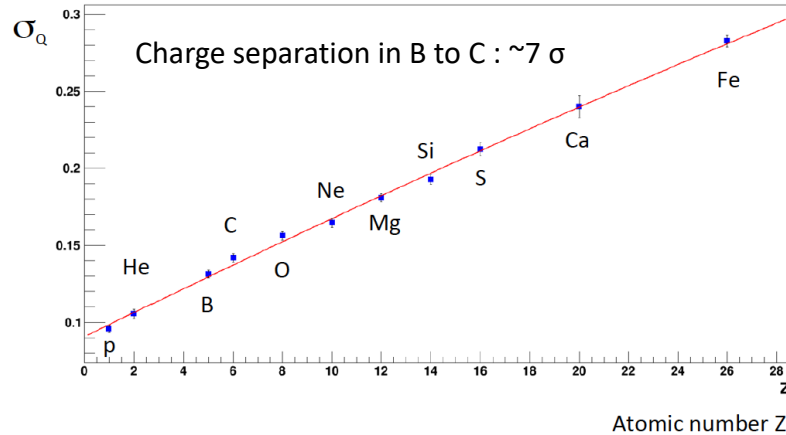
# Hadrons



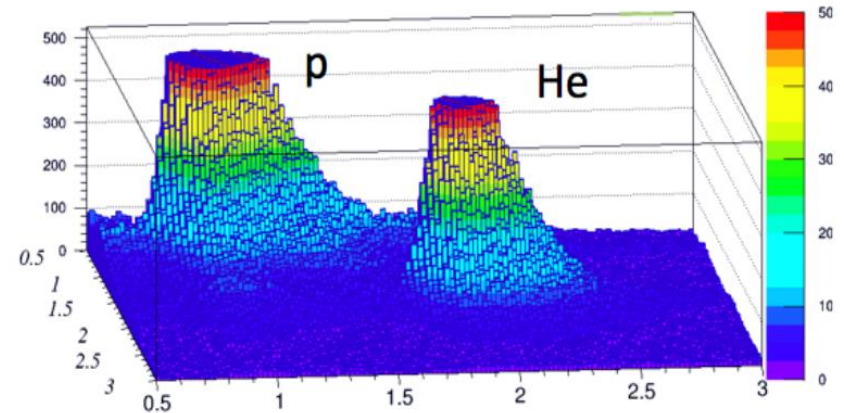
# Preliminary Nuclei Measurements (p, He, Z ≤ 8)

P.S.Marrocchesi et al.,  
ICRC 2017, PoS 205.

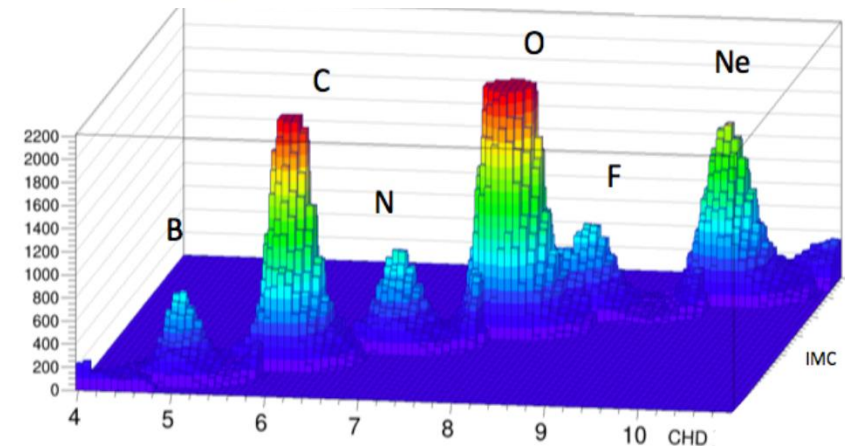
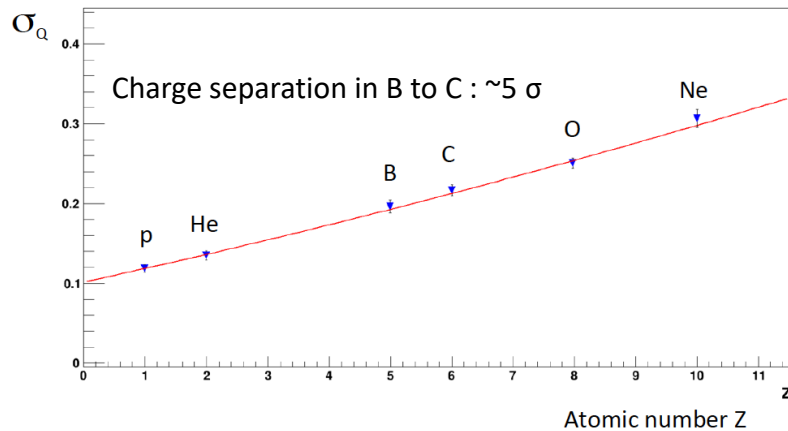
### CHD charge resolution (2 layers combined) vs. Z



### Charge resolution combined CHD+IMC



### Charge resolution using multiple dE/dx measurements from the IMC scintillating fibers



\*) Plots are truncated to clearly present the separation.

Non-linear response to  $Z^2$  is corrected both in CHD and IMC using a model.

A clear separation between p, He, up to  $Z=8$ , can be seen from CHD+IMC data analysis.



# Preliminary Flux of Primary Components

Y. Akaike et al., E+CRS 2018

Flux measurement:

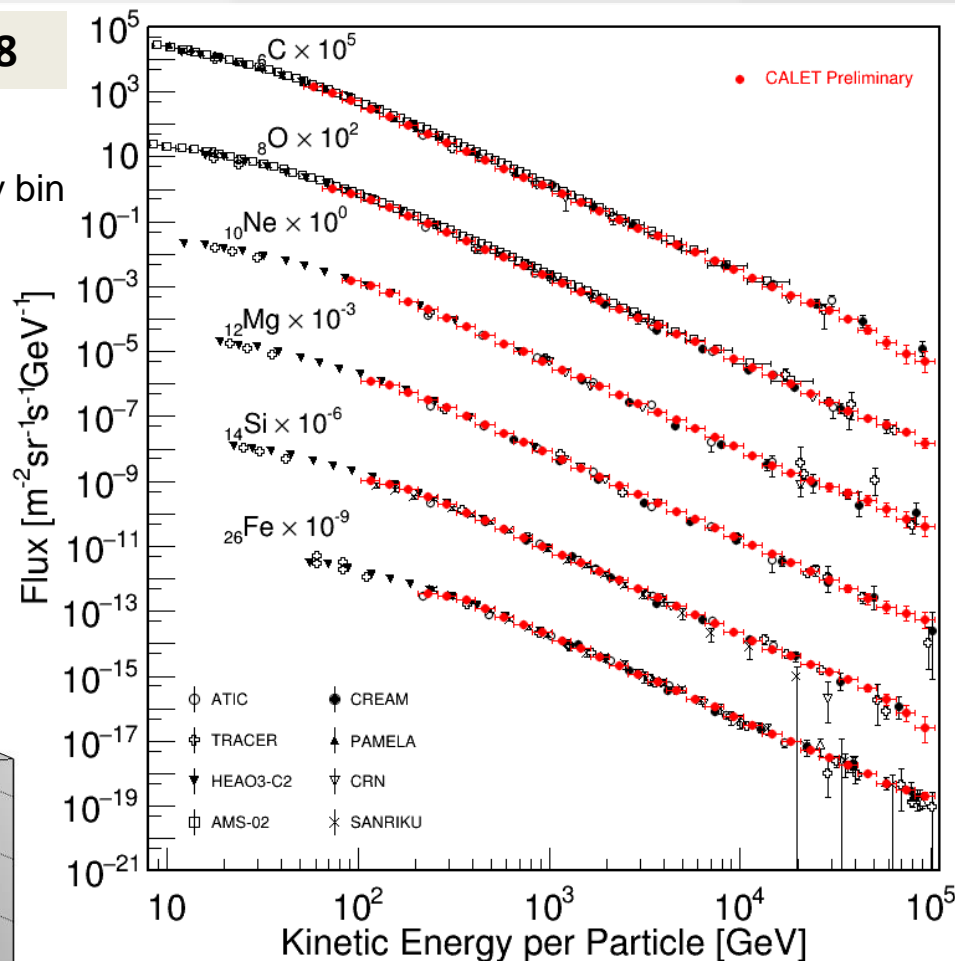
$$\Phi(E) = \frac{N(E)}{S\Omega\varepsilon(E)T\Delta E}$$

$N(E)$ : Events in unfolded energy bin  
 $S\Omega$ : Geometrical acceptance  
 $T$ : Live time  
 $\varepsilon(E)$ : Efficiency  
 $\Delta E$ : Energy bin width

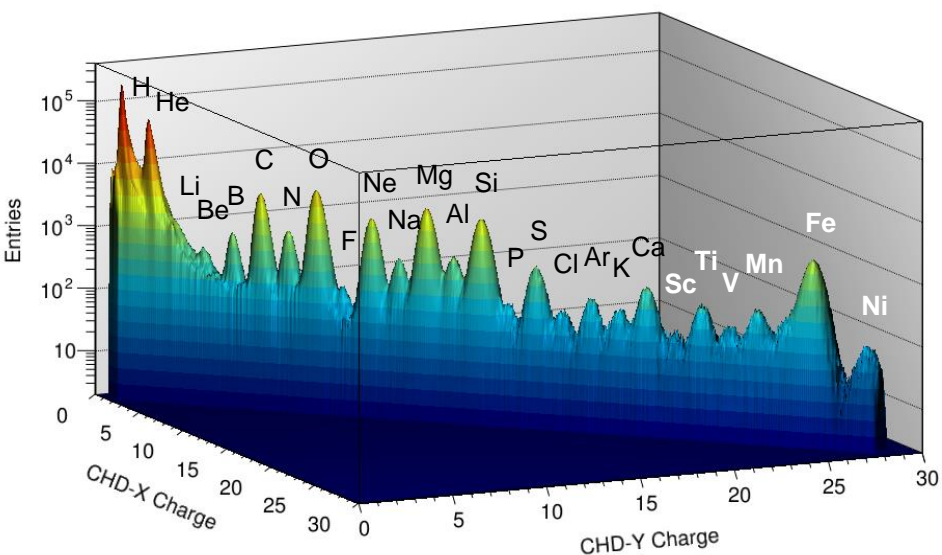
Observation period:

2015.10.13 – 2018.5.31 (962 days)

Selected events: ~5.6 million for C-Fe



Charge Separation only with CHD  
 Clear separation of protons, helium to iron and nickel (up to Z=40).

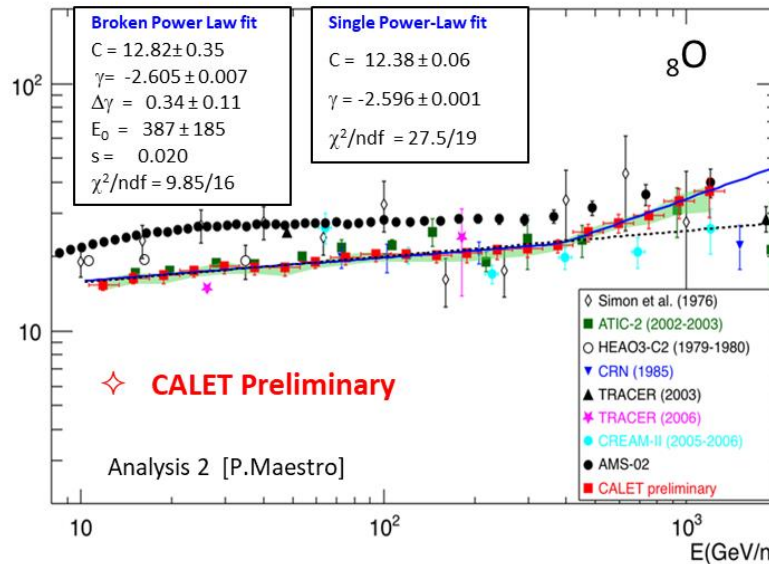
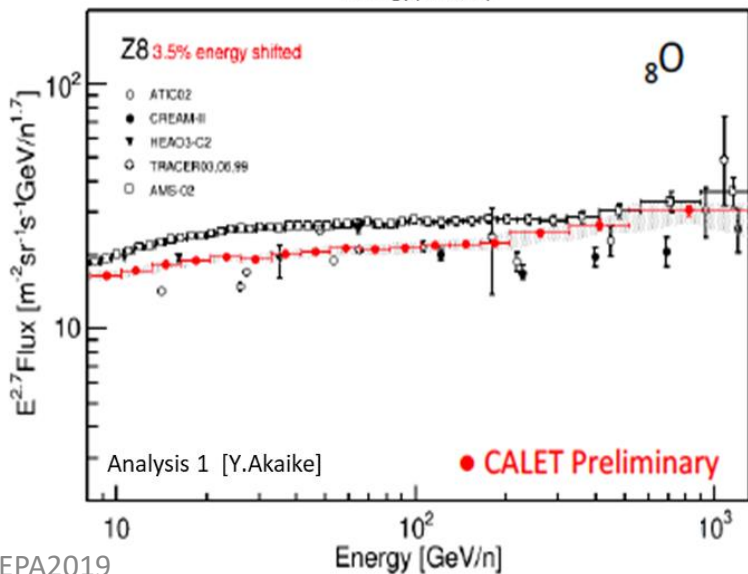
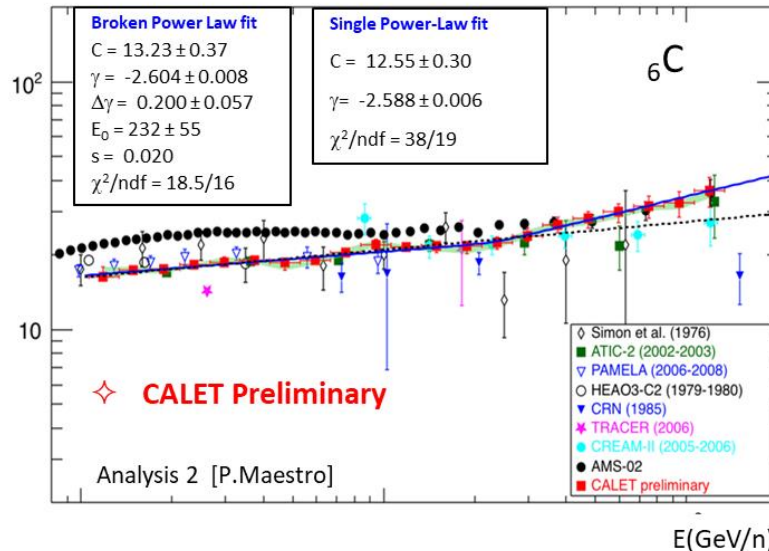
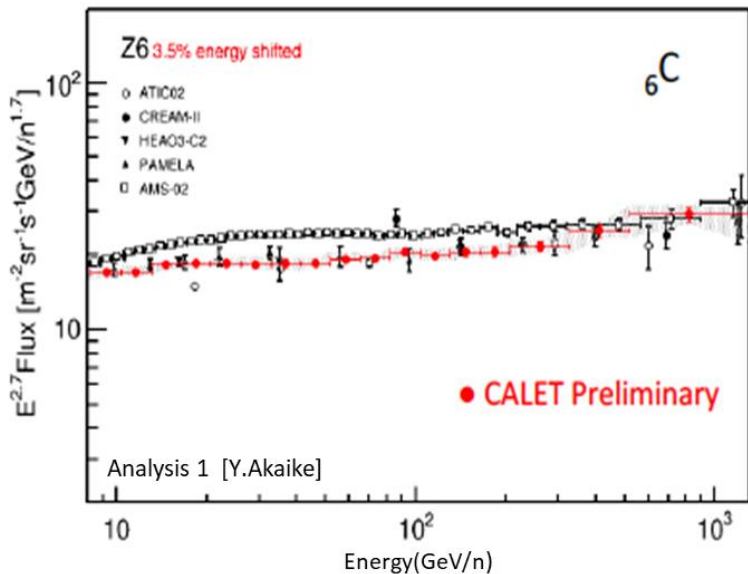




# Preliminary Energy Spectra of Carbon and Oxygen

(2 independent CALET analyses)

P. Maestro et al., COSPAR2018



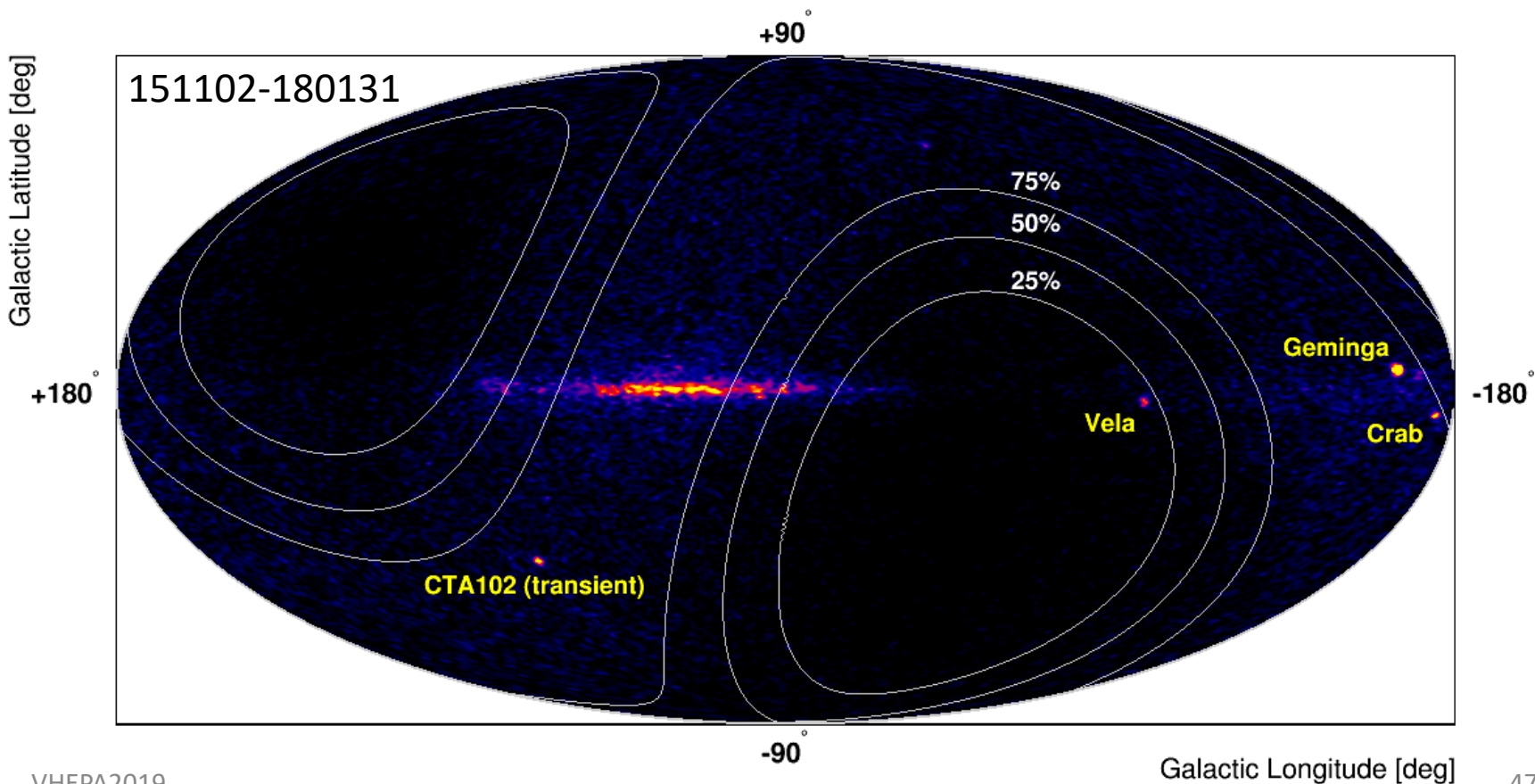
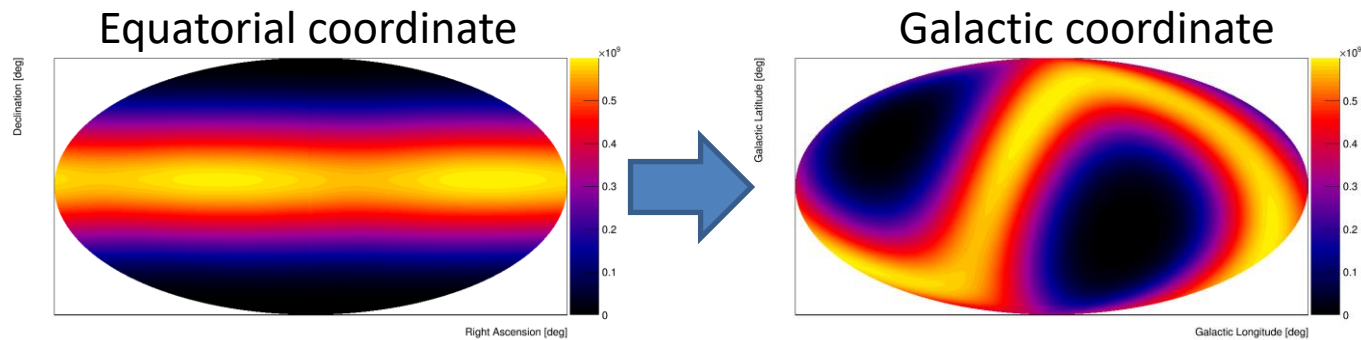
# Gamma-Rays

O.Adriani et al. (CALET Collab.), ApJL 829 (2016) L20.  
O.Adriani et al. (CALET Collab.), ApJ 863 (2018) 160.  
N.Cannady, Y.Asaoka et al. (CALET Collab.),  
ApJS 238 (2018) 5.



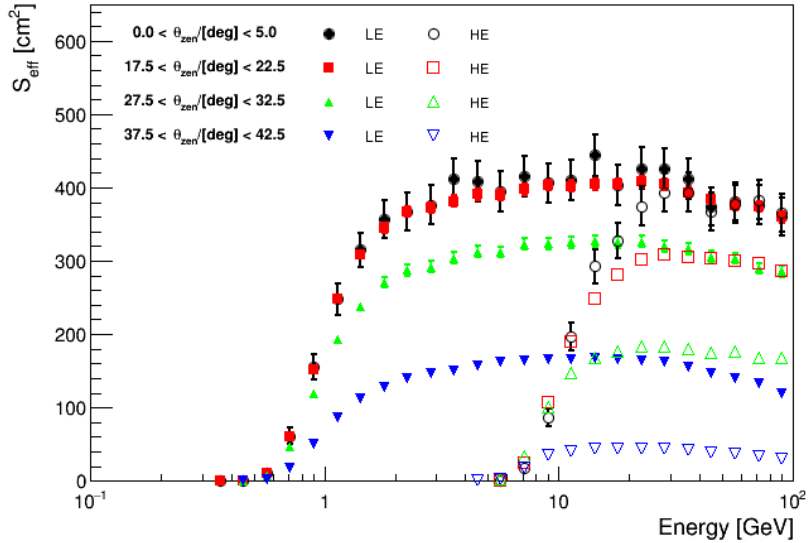
# CALET Sky Map w/ LE- $\gamma$ Trigger ( $E > 1\text{GeV}$ )

While exposure is not uniform, we have clearly identified the galactic plane and bright GeV sources.

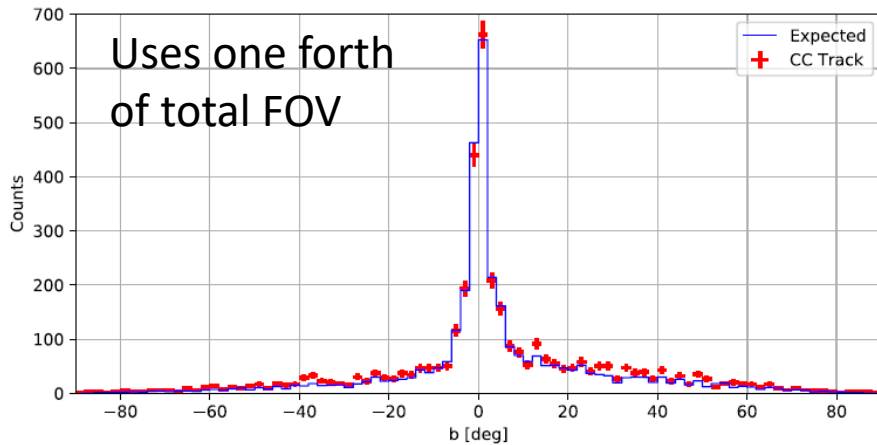




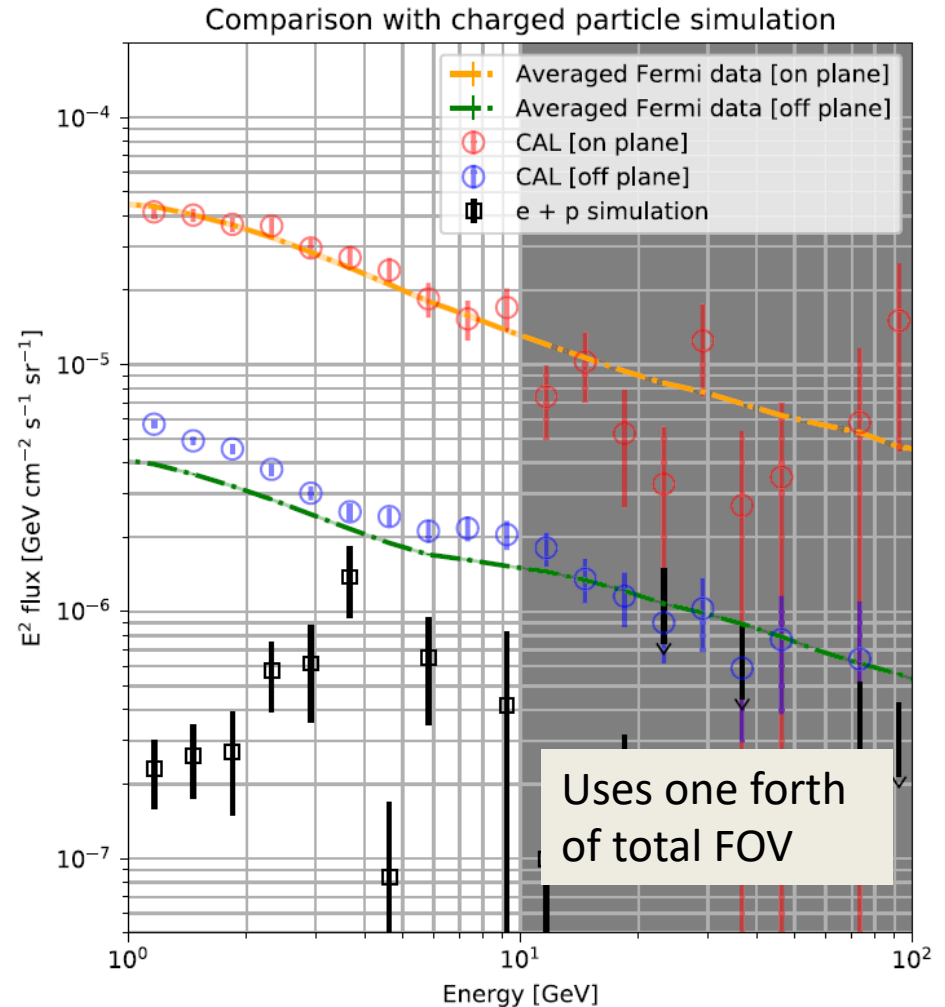
# Effective Area and $\gamma$ -ray Flux from On/Off Plane



Effective area as a function of energy. Four representing zenith angle ranges are shown.



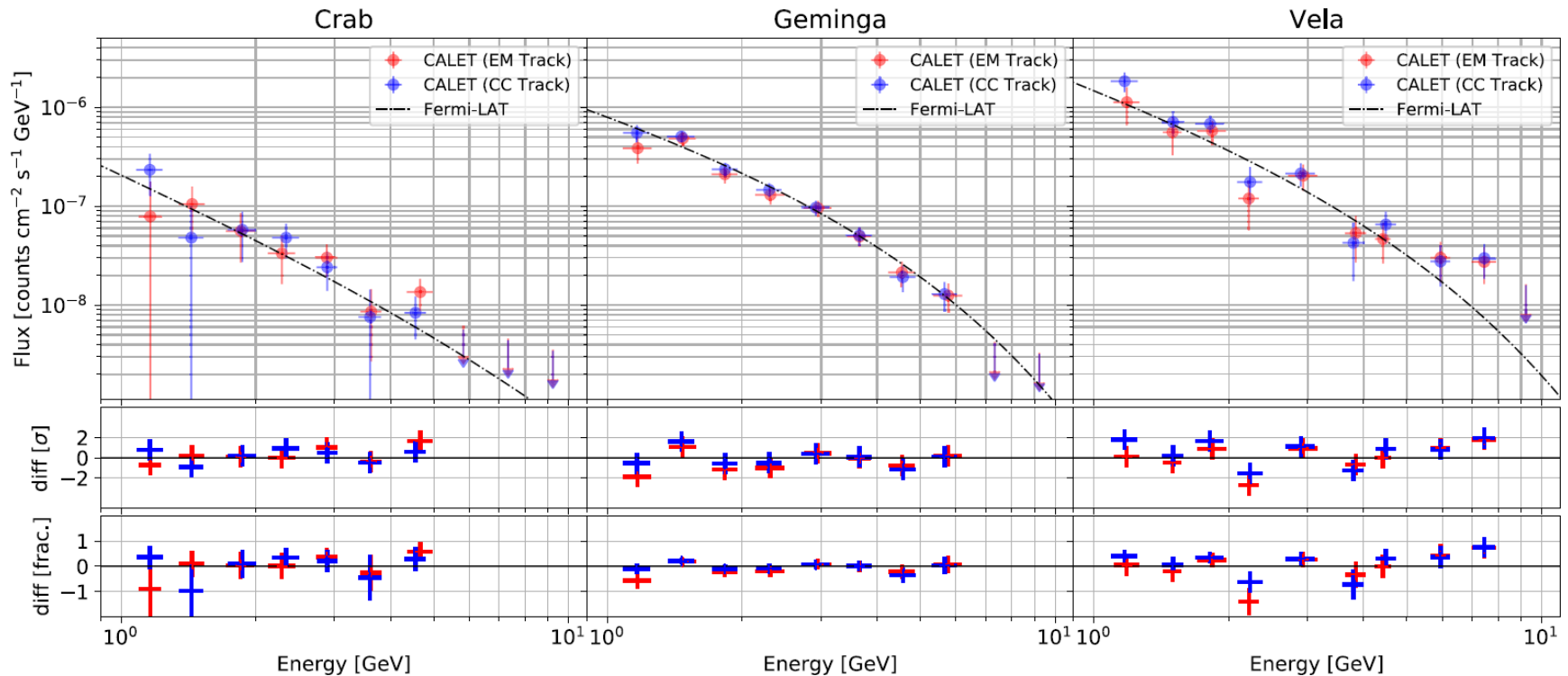
Analysis methodology, performance:  
 N.Cannady, Y.Asaoka et al.  
 (CALET Collab.), ApJS 238 (2018) 5.







# Bright Point-Source Spectra



- The observed point source spectra are well consistent with Fermi-LAT's parameterizations.
- Point Spread Function (PSF) and absolute pointing accuracy (~0.1deg) were validated, too, using bright point source data.



# CALET UPPER LIMITS ON X-RAY AND GAMMA-RAY COUNTERPARTS OF GW 151226

Astrophysical Journal Letters 829:L20(5pp), 2016 September 20

The CGBM covered 32.5% and 49.1% of the GW 151226 sky localization probability in the 7 keV - 1 MeV and 40 keV - 20 MeV bands respectively. We place a 90% upper limit of  $2 \times 10^{-7}$  erg cm<sup>-2</sup> s<sup>-1</sup> in the 1 - 100 GeV band where CAL reaches 15% of the integrated LIGO probability (~1.1 sr). The CGBM 7  $\sigma$  upper limits are  $1.0 \times 10^{-6}$  erg cm<sup>-2</sup> s<sup>-1</sup> (7-500 keV) and  $1.8 \times 10^{-6}$  erg cm<sup>-2</sup> s<sup>-1</sup> (50-1000 keV) for one second exposure. Those upper limits correspond to the luminosity of  $3-5 \times 10^{49}$  erg s<sup>-1</sup> which is significantly lower than typical short GRBs.

## CGBM light curve at the moment of the GW151226 event

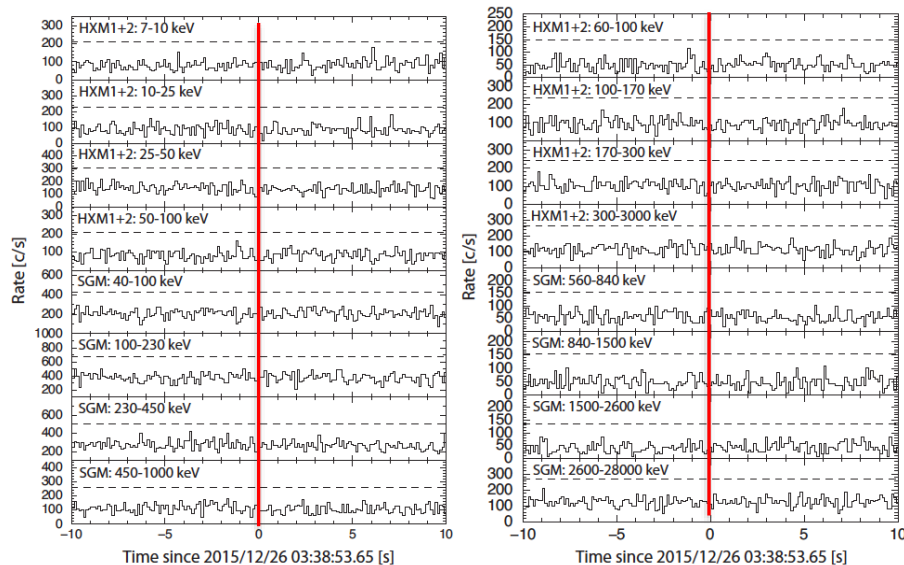


Figure 1. The CGBM light curves in 0.125 s time resolution for the high-gain data (left) and the low-gain data (right). The time is offset from the LIGO trigger time of GW 151226. The dashed-lines correspond to the 5  $\sigma$  level from the mean count rate using the data of  $\pm 10$  s.

## Upper limit for gamma-ray burst monitors and Calorimeter

HXM: 7-500 keV

SGM: 50-1000 keV

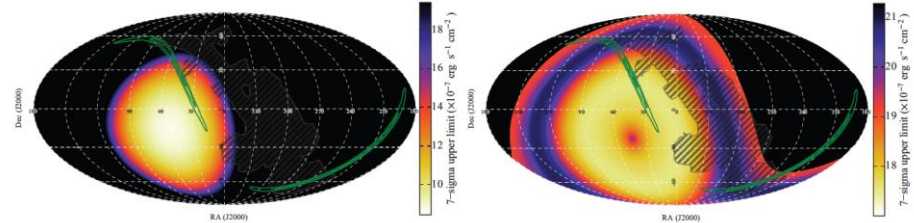


Figure 2. The sky maps of the 7  $\sigma$  upper limit for HXM (left) and SGM (right). The assumed spectrum for estimating the upper limit is a typical BATSE S-GRBs (see text for details). The energy bands are 7-500 keV for HXM and 50-1000 keV for SGM. The GW 151226 probability map is shown in green contours. The shadow of ISS is shown in black hatches.

Calorimeter:  
1-100 GeV

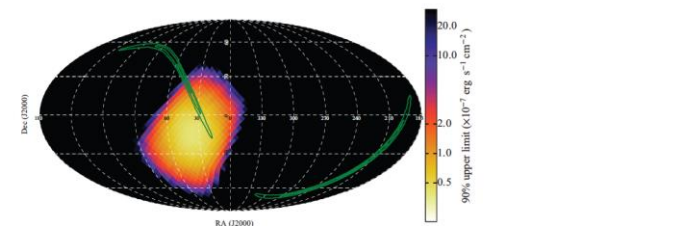


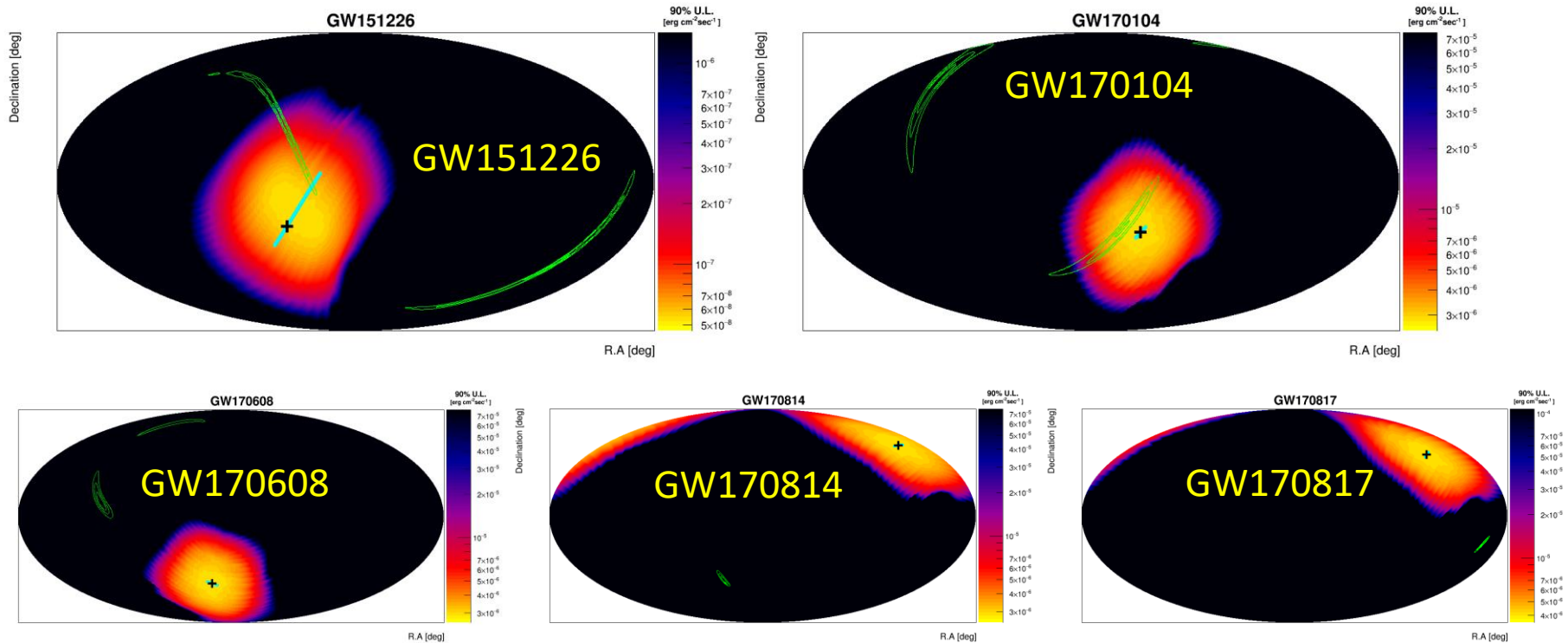
Figure 3. The sky map of the 90% upper limit for CAL in the 1-100 GeV band. A power-law model with a photon index of  $-2$  is used to calculate the upper limit. The GW 151226 probability map is shown in green contours.



# Complete Search Results for GW Events during O1&O2

O.Adriani et al. (CALET Collaboration), ApJ 863 (2018) 160.

- CALET was not operational, yet, at the time of GW150914.
- For GW151226, we set 90% C.L. limit of  $9.3 \times 10^{-8} \text{ erg cm}^{-2} \text{ s}^{-1}$  (1-10GeV) covering 15% of the summed LIGO probabilities in the time window [T0-525s, T0+211s] (LE trigger).
- For GW170104, we set 90% C.L. limit of  $8.3 \times 10^{-6} \text{ erg cm}^{-2} \text{ s}^{-1}$  (10-100GeV) covering 30% of the summed LIGO probabilities in the time window [T0-60s, T0+60s] (HE trigger).
- Unfortunately, other GW events (GW170608, GW170814, GW170817) occurred during O2 are all out of the CALET-CAL FOV.





# Complete Search Results for GW Events during O1&O2

**O.Adriani et al. (CALET Collaboration), ApJ 863 (2018) 160.**

- CALET was not operational, yet, at the time of GW150914.
- For GW151226, we set 90% C.L. limit of  $9.3 \times 10^{-8} \text{ erg cm}^{-2} \text{ s}^{-1}$  (1-10GeV) covering 15% of the summed LIGO probabilities in the time window  $[T_0-525\text{s}, T_0+211\text{s}]$  (LE trigger).
- For GW170104, we set 90% C.L. limit of  $8.3 \times 10^{-6} \text{ erg cm}^{-2} \text{ s}^{-1}$  (10-100GeV) covering 30% of the summed LIGO probabilities in the time window  $[T_0-60\text{s}, T_0+60\text{s}]$  (HE trigger).
- Unfortunately, other GW events (GW170608, GW170814, GW170817) occurred during O2 are all out of the CALET-CAL FOV.

**Table 1**

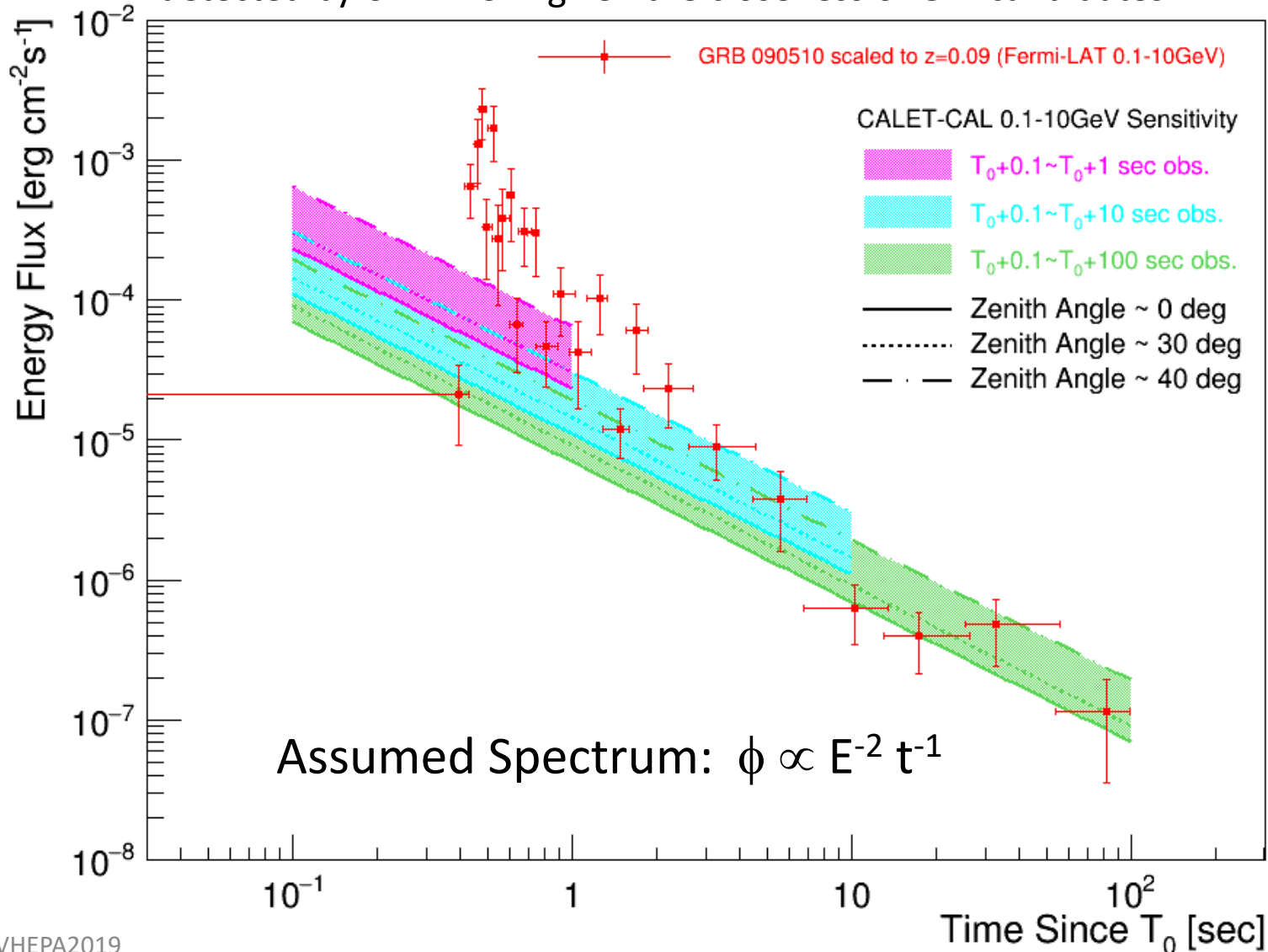
Summary of *CALET* Observations of Gravitational Events Reported by the Virgo and LIGO Scientific Collaborations (BH: black hole, NS: Neutron Star) and Representative Results from *CALET* Observation (See the Text for Other Time Windows)

| GW event | Time<br>$T_0$<br>(UTC)  | Location<br>area<br>(deg <sup>2</sup> ) | Luminosity<br>distance<br>(Mpc) | Event<br>Type | References | <i>CALET</i> Results [Time Window] |                               |   |                                      |
|----------|-------------------------|---|---------------------------------|---------------|------------|------------------------------------|-------------------------------|---|--------------------------------------|
|          |                         |   |                                 |               |            | Mode                               | Summed<br>LIGO<br>probability | Upper Limits (90% C.L.)   |                                      |
|          |                         |   |                                 |               |            |                                    |                               | Energy Flux<br>(erg cm <sup>-2</sup> s <sup>-1</sup> )                                    | Luminosity<br>(erg s <sup>-1</sup> ) |
| GW150914 | 2015 Sep 14<br>09:50:45 | 600                                     | $440_{-180}^{+160}$             | BH–BH         | (a)        |                                    |                               | Before operation  |                                      |
| GW151226 | 2015 Dec 26<br>03:38:53 | 850                                     | $440_{-190}^{+180}$             | BH–BH         | (b)        | LE                                 | 15%                           | $[T_0 - 525 \text{ s}, T_0 + 211 \text{ s}]$<br>$9.3 \times 10^{-8}$ $2.3 \times 10^{48}$ |                                      |
| GW170104 | 2017 Jan 04<br>10:11:58 | 1200                                    | $880_{-390}^{+450}$             | BH–BH         | (c)        | HE                                 | 30%                           | $[T_0 - 60 \text{ s}, T_0 + 60 \text{ s}]$<br>$6.4 \times 10^{-6}$ $6.2 \times 10^{50}$   |                                      |
| GW170608 | 2017 Jun 08<br>02:01:16 | 520                                     | $340_{-140}^{+140}$             | BH–BH         | (d)        | HE                                 |                               | $[T_0 - 60 \text{ s}, T_0 + 60 \text{ s}]$<br>Out of FOV                                  |                                      |
| GW170814 | 2017 Aug 14<br>10:30:43 | 60                                      | $540_{-210}^{+130}$             | BH–BH         | (e)        | HE                                 |                               | $[T_0 - 60 \text{ s}, T_0 + 60 \text{ s}]$<br>Out of FOV                                  |                                      |
| GW170817 | 2017 Aug 17<br>12:41:04 | 28                                      | $40_{-14}^{+8}$                 | NS–NS         | (f)        | HE                                 |                               | $[T_0 - 60 \text{ s}, T_0 + 60 \text{ s}]$<br>Out of FOV                                  |                                      |



# CALET Sensitivity to GeV Gamma-Rays

Short GRBs accompanied by GeV gamma-ray emissions could be detected by CALET-CAL given the closeness of GW candidates.





# Summary and Future Prospects

- CALET was successfully launched on Aug. 19, 2015, and the detector is being very stable for observation since Oct. 13, 2015.
- **As of October 31, 2018, total observation time is 1115 days with live time fraction to total time close to 84%. Nearly 730 million events are collected with high energy trigger ( $E > 10$  GeV)**
- Careful calibrations have been adopted by using “MIP” signals of the non-interacting p & He events, and the linearity in the energy measurements up to  $10^6$  MIPs is established by using observed events.
- **All electron spectrum has been extended in statistics and in the energy range up to 4.8 TeV. This result is published in PRL again on June 2018.**
- **Preliminary analysis of nuclei have successfully been carried out to obtain the energy spectra in the energy range: Protons in 55 GeV~22 TeV, Ne-Fe in 500 GeV~100 TeV.**
- CALET's CGBM detected nearly 60 GRBs (~20 % short GRB among them ) per year in the energy range of 7 keV-20 MeV, as expected (not included in this talk). Follow-up observation of the GW events is carried out and published in ApJL.
- **GW counterpart searches with CALET calorimeter were extended to cover the whole LIGO/Virgo O2 and published in ApJ (August 2018). In addition, onboard performance of gamma-ray observation is published in ApJS (September 2018).**
- The so far excellent performance of CALET and the outstanding quality of the data suggest that a 5-year observation period is likely to provide a wealth of new interesting results.